Dark Matter

ASTR 333/433

TODAY

Tully-Fisher

Rotation Curve Shapes

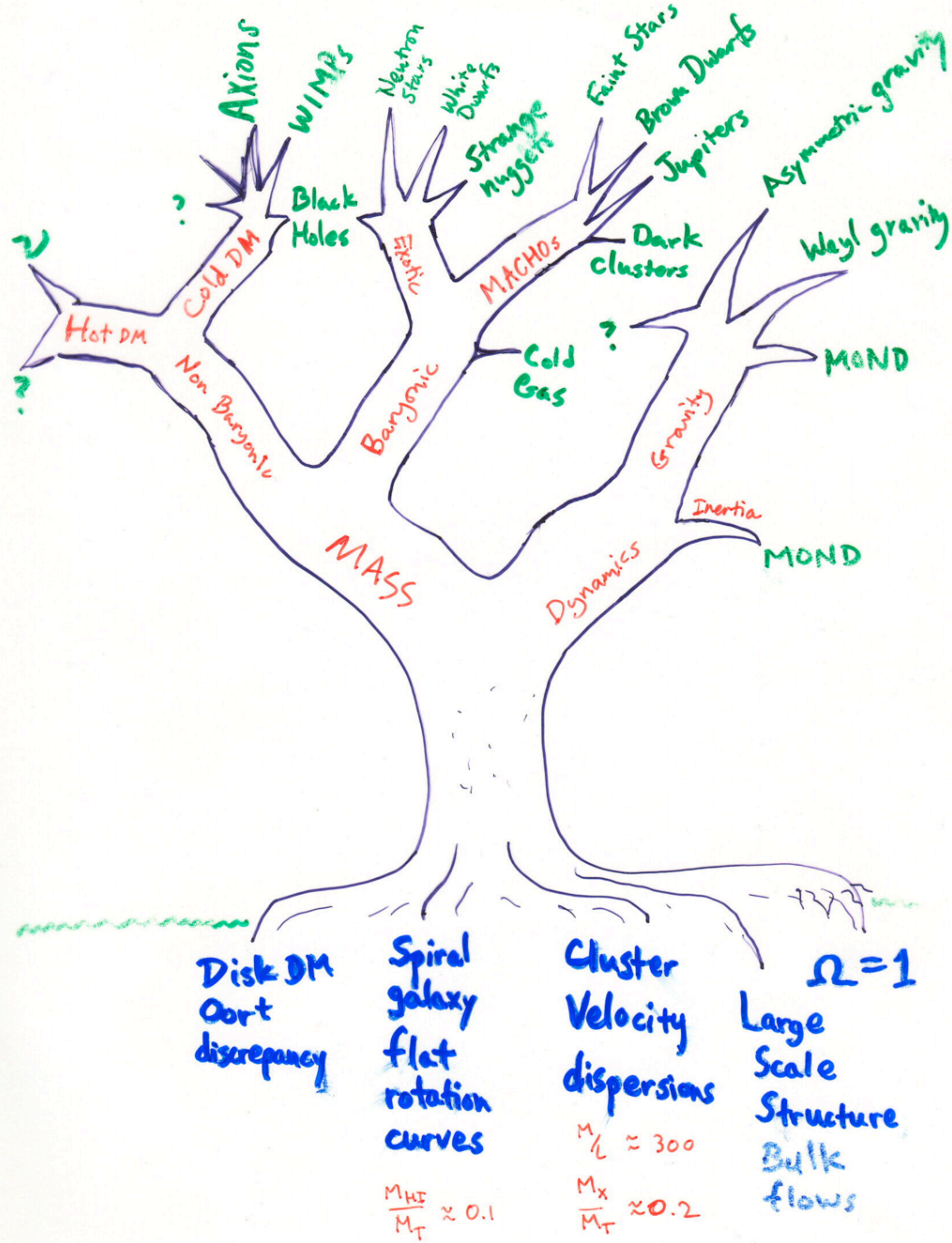

Empirical Laws of Galactic Rotation

- Flat rotation curves (Rubin-Bosma Law)

  Rotation curves tend asymptotically towards a constant rotation velocity that persists to indefinitely large radii: $V(R \to \infty) \to V_f$

- Tully-Fisher relation (Luminous, Stellar Mass, and Baryonic TF relations)

  The baryonic mass of galaxies scales as the fourth power of the flat rotation velocity: $M_b = AV_f^4$

- Central density relation (lower surface brightness galaxies exhibit larger mass discrepancies)

  The central dynamical surface densities of galaxies is related to their central surface brightnesses: $\Sigma_{dyn}(R \to 0) = f[\Sigma_*(R \to 0)]$

- Renzo's rule (Sancisi's Law)

  "For any feature in the luminosity profile there is a corresponding feature in the rotation curve and vice versa." (Sancisi 2004).

- Radial acceleration relation

  The observed centripetal acceleration is related to that predicted by the observed distribution of baryons: $\mathrm{g}_{\mathrm{obs}} = \mathcal{F}(\mathrm{g}_{\mathrm{bar}})$

stellar population models

Typically, redder colors mean higher mass-to-light ratios

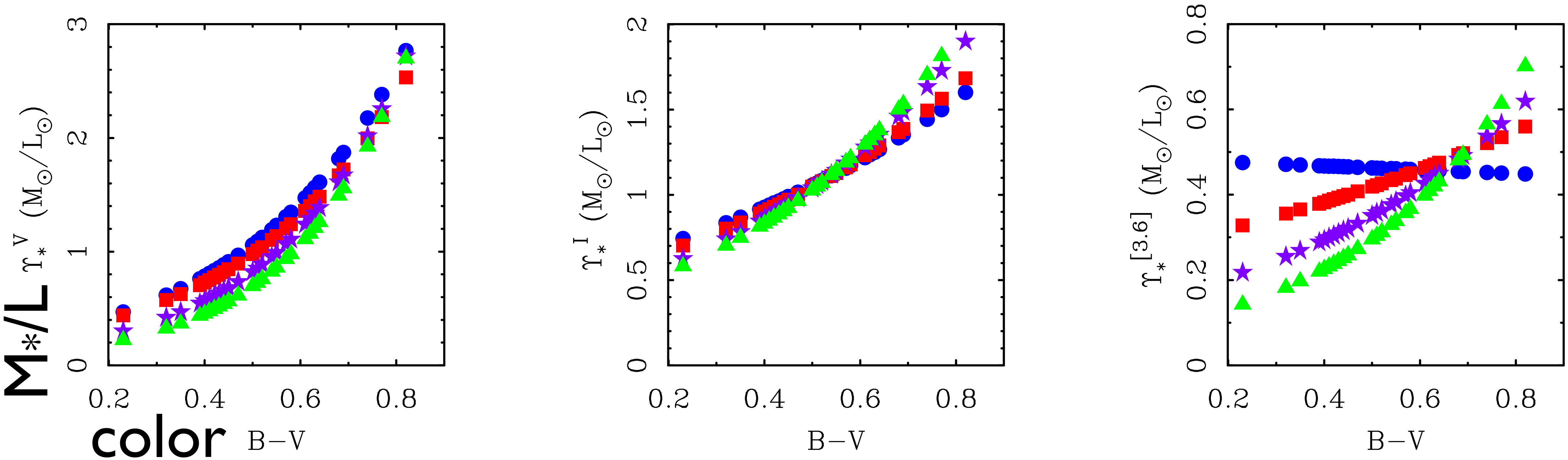

$$\log\left(\frac{M_*}{L_i}\right) = a_i + b_i(B-V)$$

Table 7
Revised CMLR

Model	a_V	b_V	α_I	β_I	$\alpha_{[3.6]}$	$\beta_{[3.6]}$	$\Upsilon_{0.6}^V$	$\Upsilon_{0.6}^I$	$\Upsilon_{0.6}^K$	$\Upsilon_{0.6}^{[3.6]}$
Bell et al. (2003)	−0.628	1.305	−0.275	0.612	−0.322	−0.007	1.43	1.24	0.61	0.47
Portinari et al. (2004)	−0.654	1.290	−0.321	0.701	−0.594	0.467	1.32	1.26	0.63	0.49
Zibetti et al. (2009)	−1.075	1.837	−0.477	1.004	−1.147	1.289	1.07	1.33	0.54	0.42
Into & Portinari (2013)	−0.900	1.627	−0.421	0.898	−0.861	0.849	1.19	1.31	0.58	0.45

Tully-Fisher relation

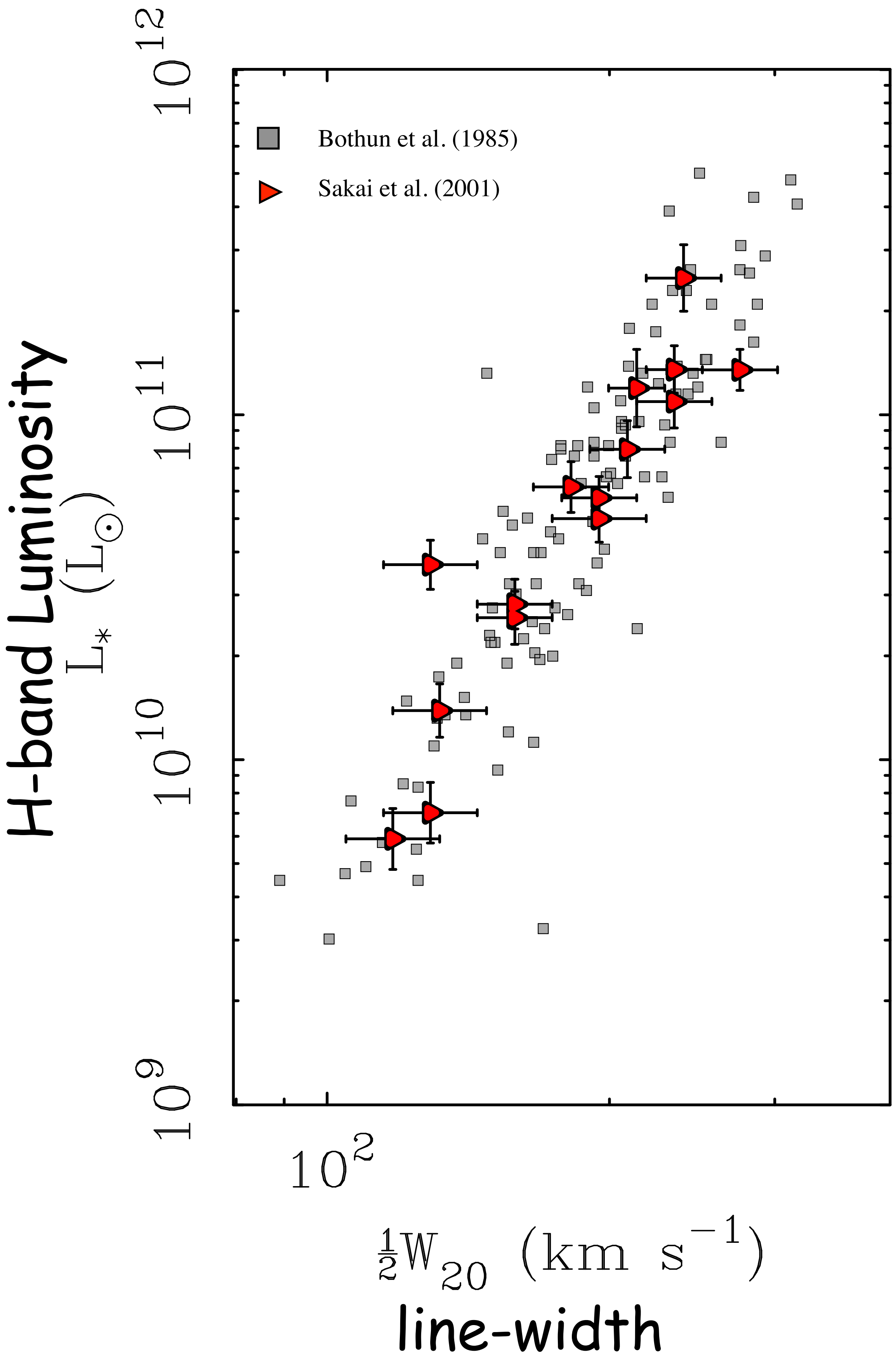

Luminosity and line-width are presumably proxies for stellar mass and rotation velocity.

Stellar Mass Tully-Fisher relation

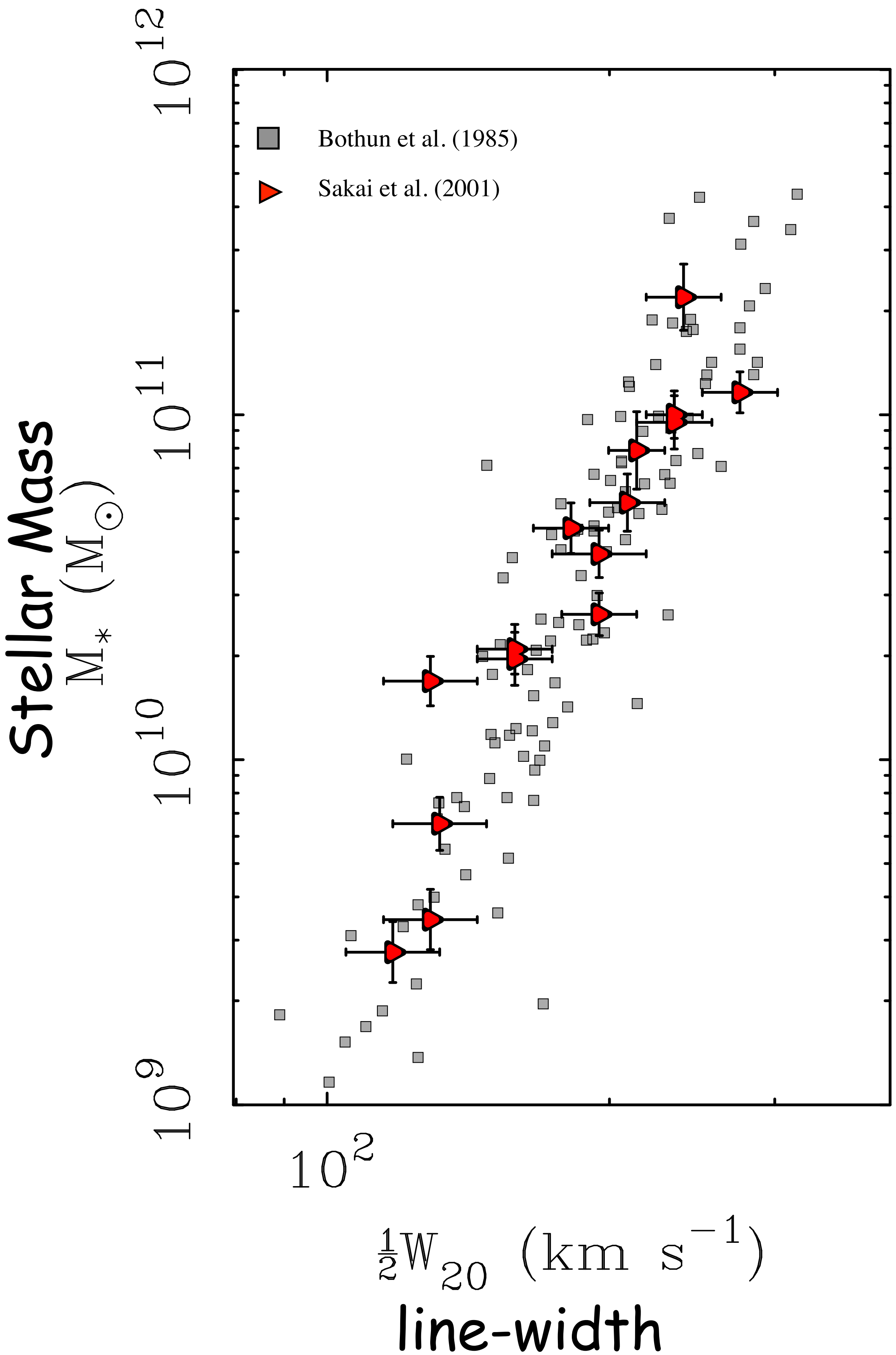

nominal M*/L (Kroupa IMF)

$$M_* = \left(\frac{M_*}{L}\right) L$$

Stellar mass TF steeper than regular TF because of the color—magnitude relation (brighter galaxies are redder) and the color—M*/L relation (redder galaxies have higher M*/L).

Stark, McGaugh, & Swaters et al. (2009)

If you want to use Vflat, you have to observe far enough out to measure it.

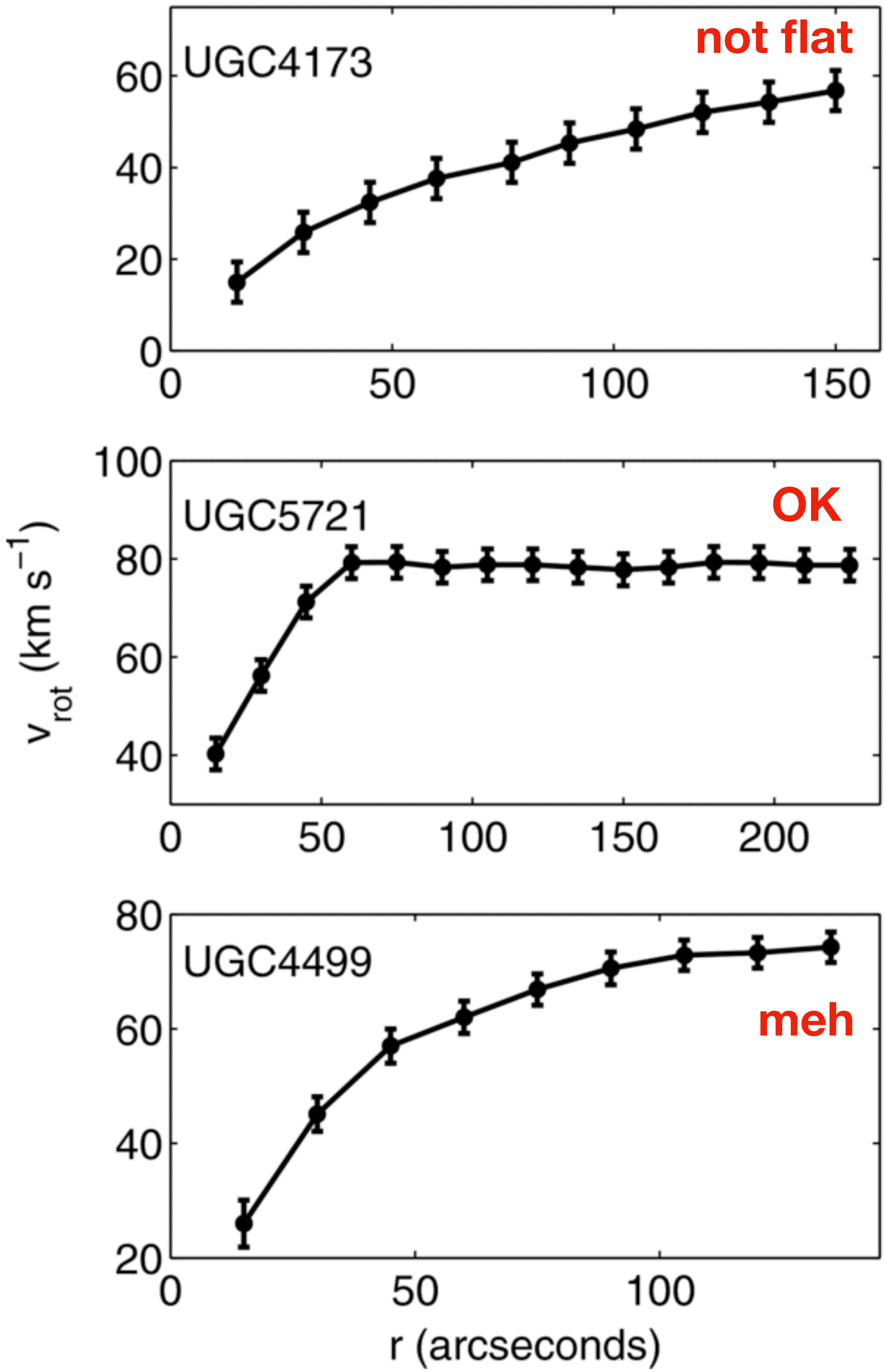

Scatter in TF increases as quality threshold weakened.

Scatter in TF relation reduced with resolved rotation curves (Verheijen 2001)

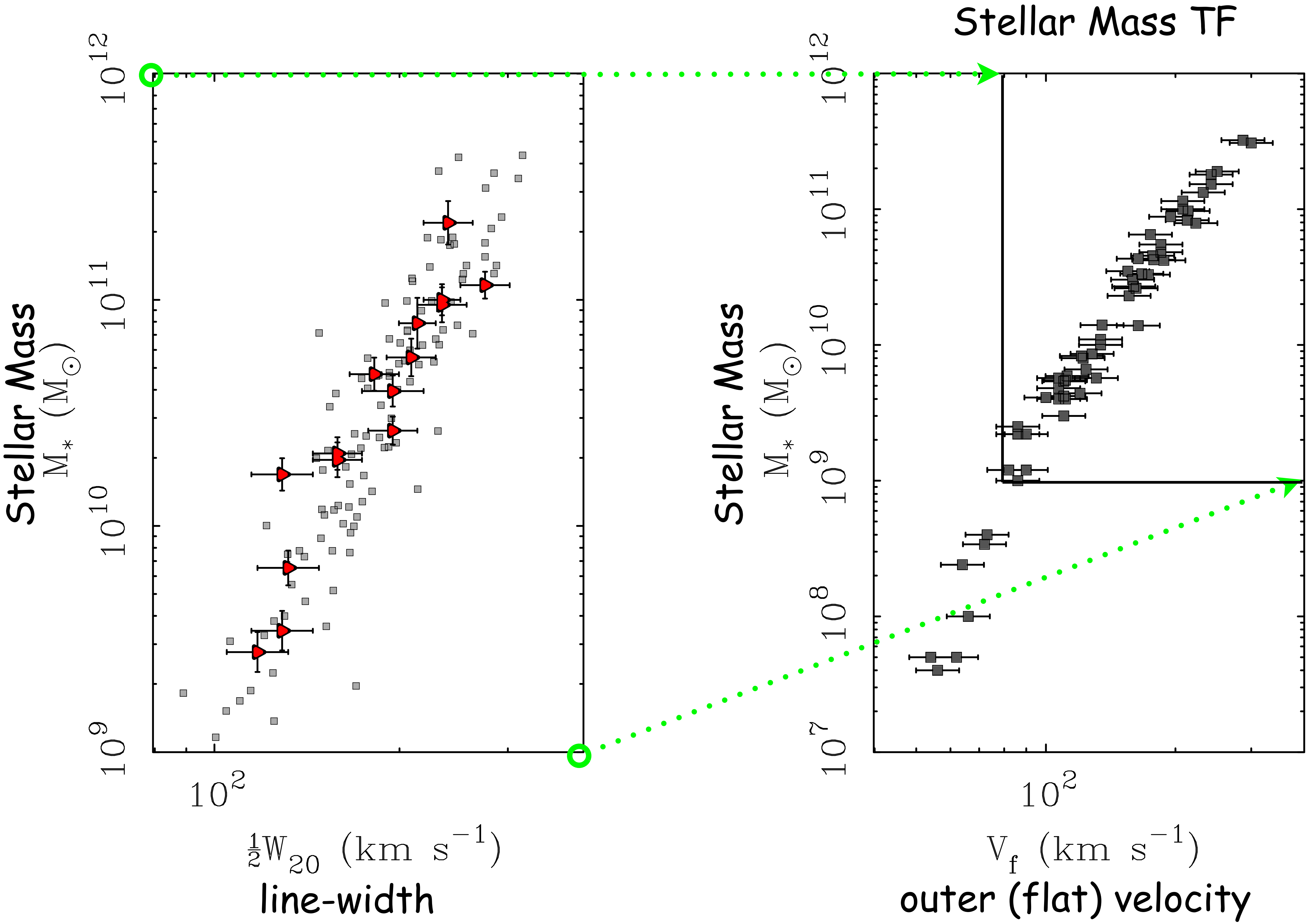

Low mass galaxies tend to fall below extrapolation of linear fit to fast rotators (Matthews, van Driel, & Gallagher 1998; Freeman 1999)

$$M_* = \left(\frac{M_*}{L}\right) L$$

Stellar Mass TF

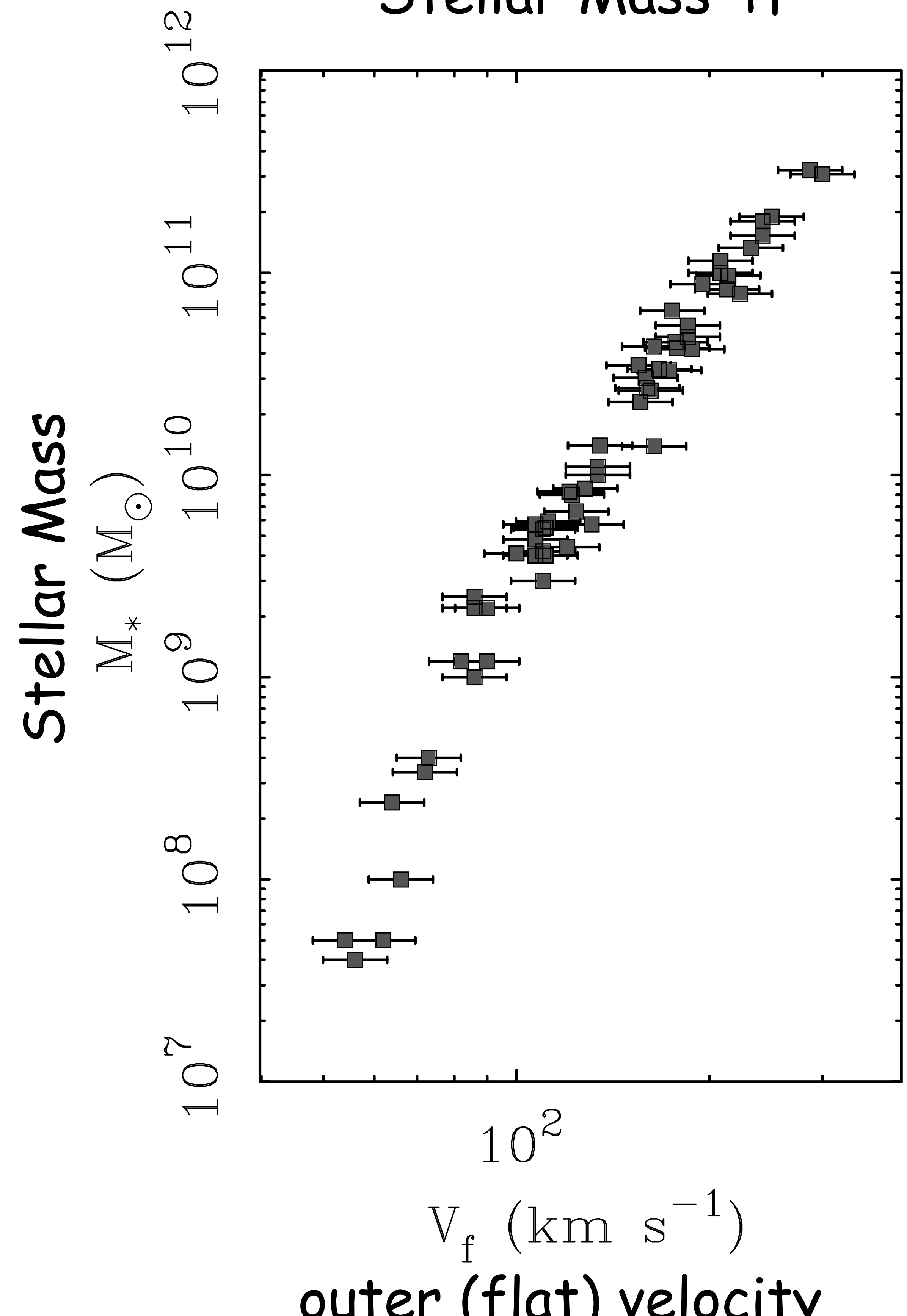

Gas mass by itself does NOT produce a good TF relation, at least for fast rotators.

$$M_g = 1.4 M_{HI}$$

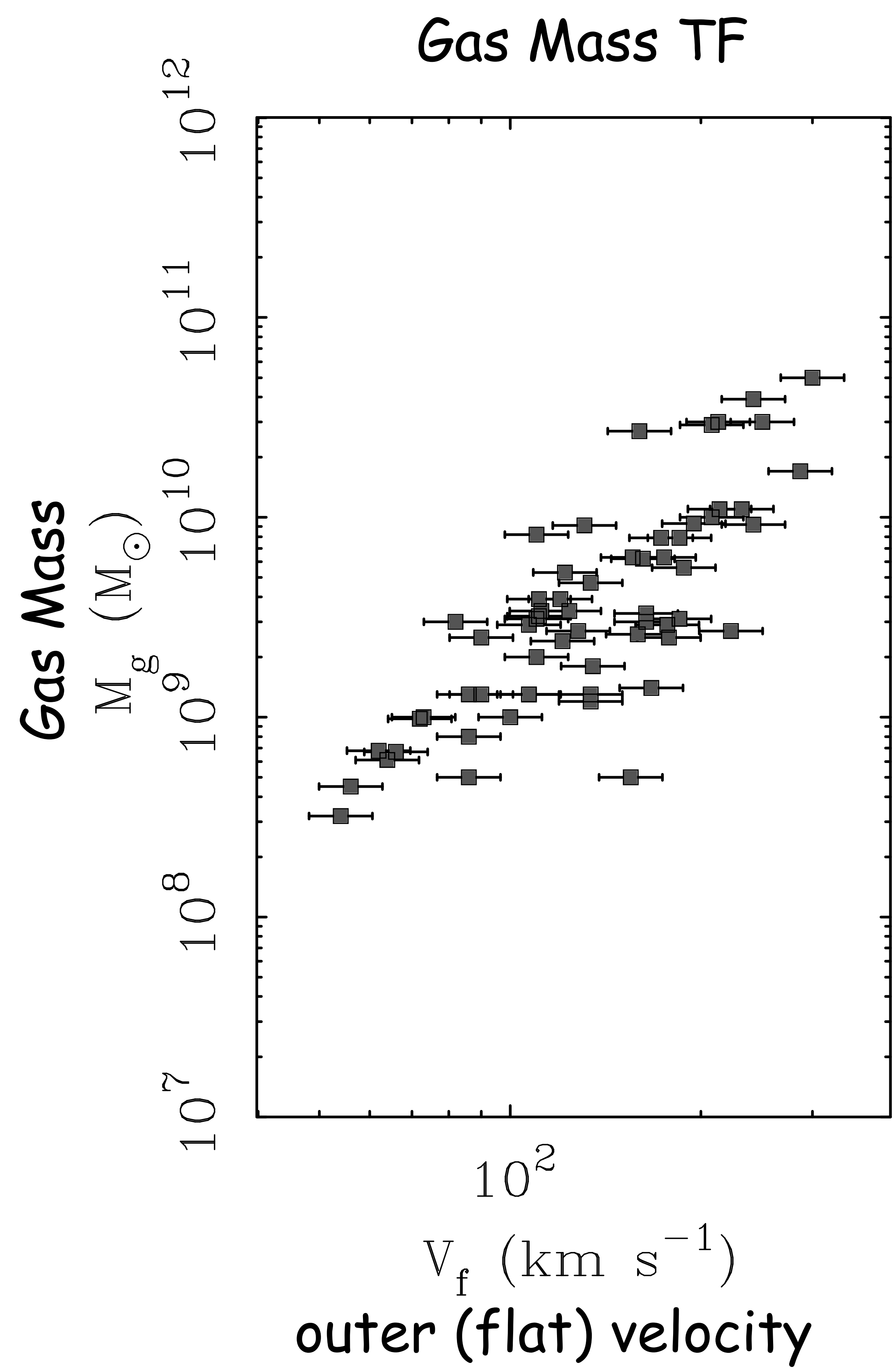

Adding gas to stellar mass restores a single continuous relation for all rotators.

$$M_b = M_* + M_g$$

Baryonic mass is the important physical quantity. It doesn't matter whether the mass is in stars or in gas.

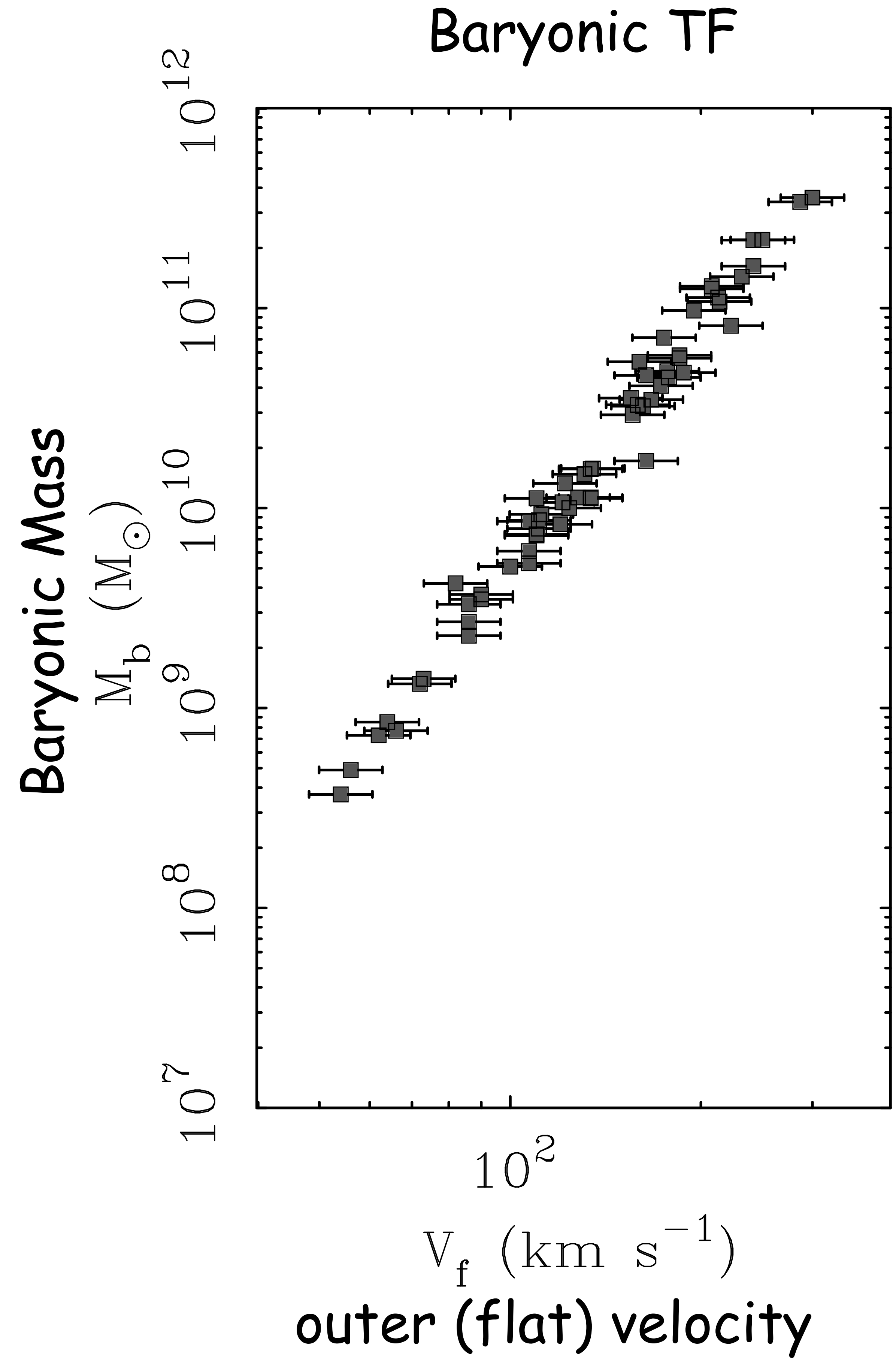

Low mass galaxies considerably expand range of the TF relation.
Gas dominated galaxies can provide absolute calibration of mass scale.

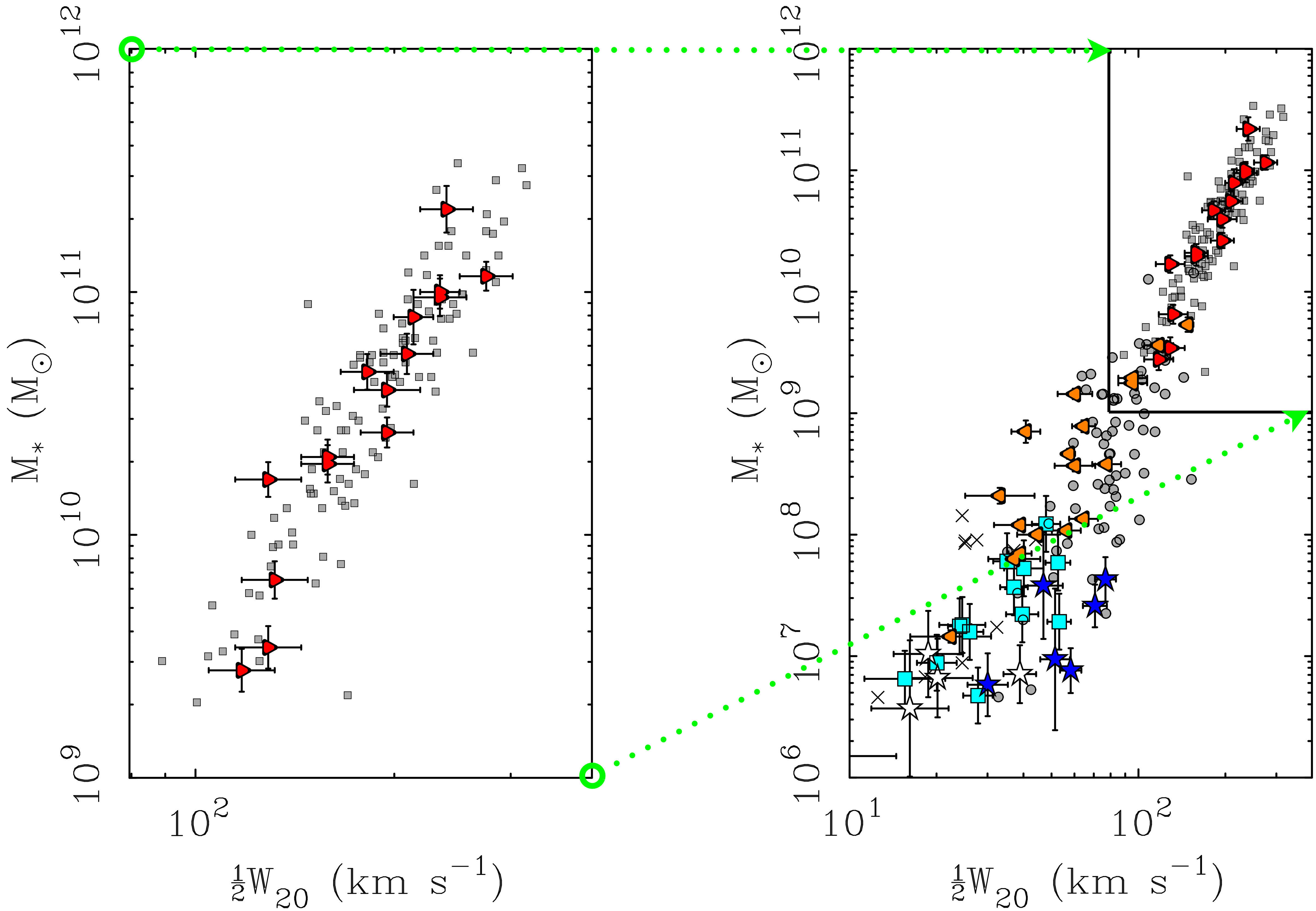

Gotta believe the data.

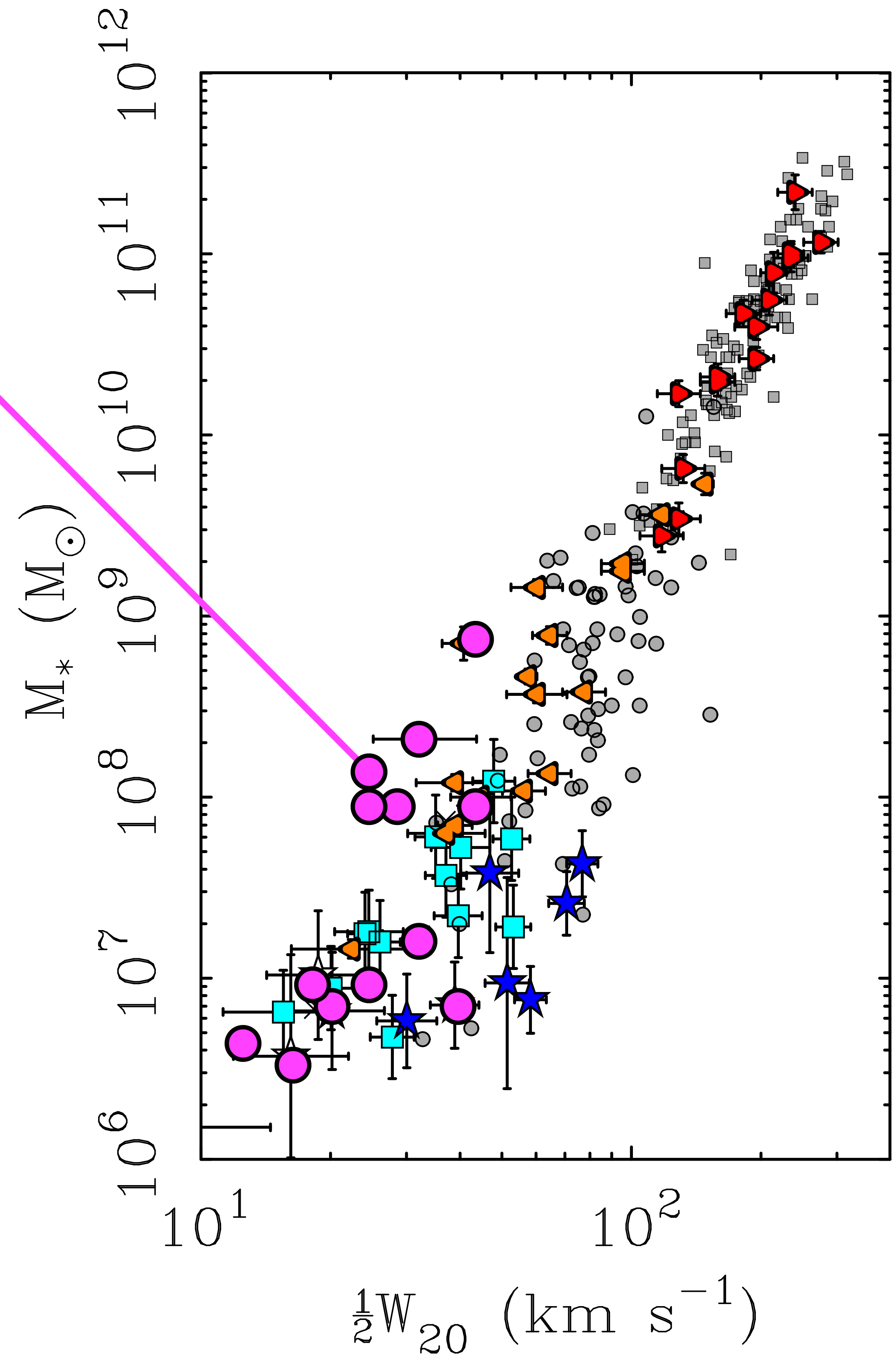

Biggest challenge for low mass systems is the inclination

e.g., Begum et al. (2008) estimate inclinations from both optical and HI morphology. Only half agree to within 12% in sin(i).

Trachternach et al. (2009)

Example low line-width, gas dominated galaxies with $M_\star < M_g$

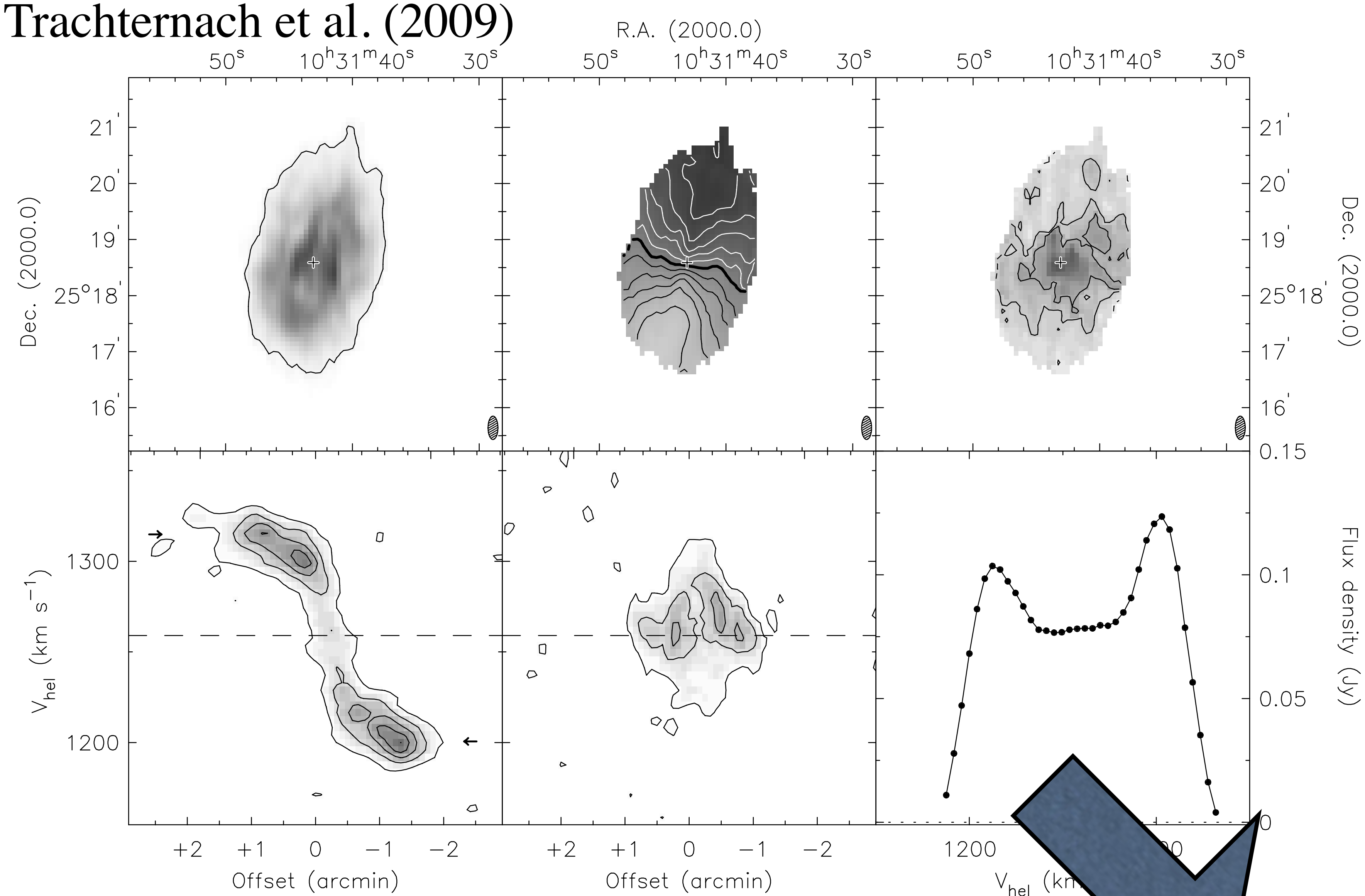

HI

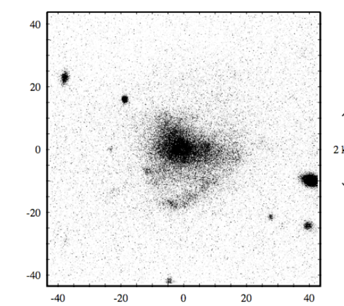

optical

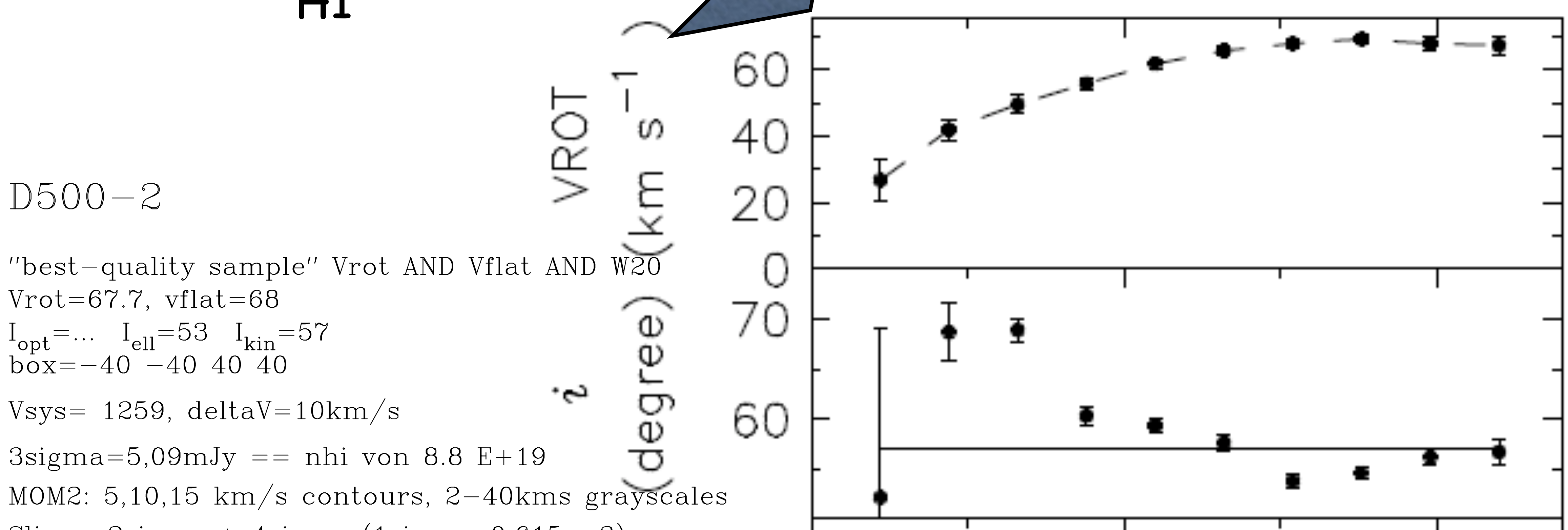

Trachternach et al. (2009)

D500-3

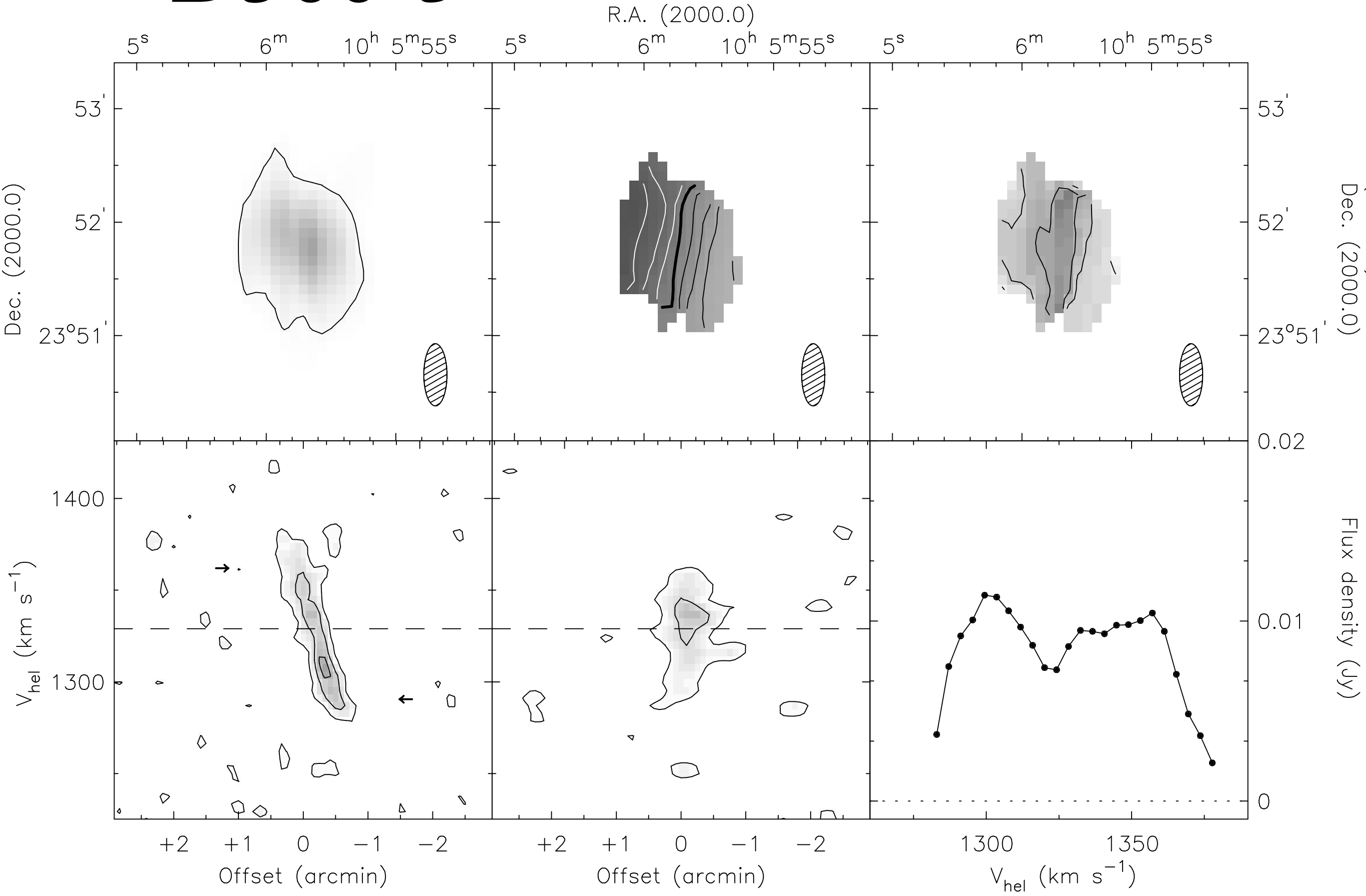

D631-7

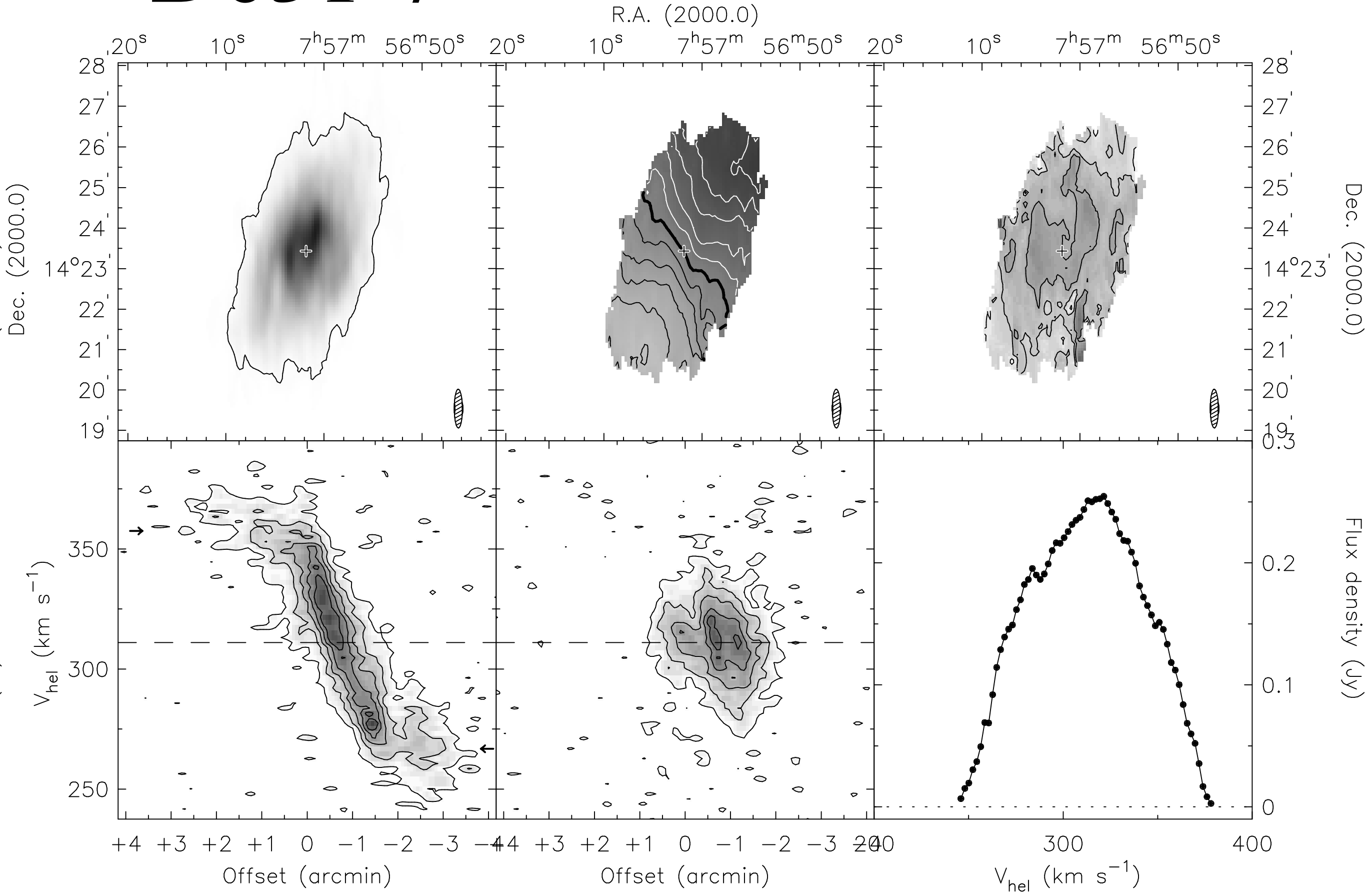

D512-2

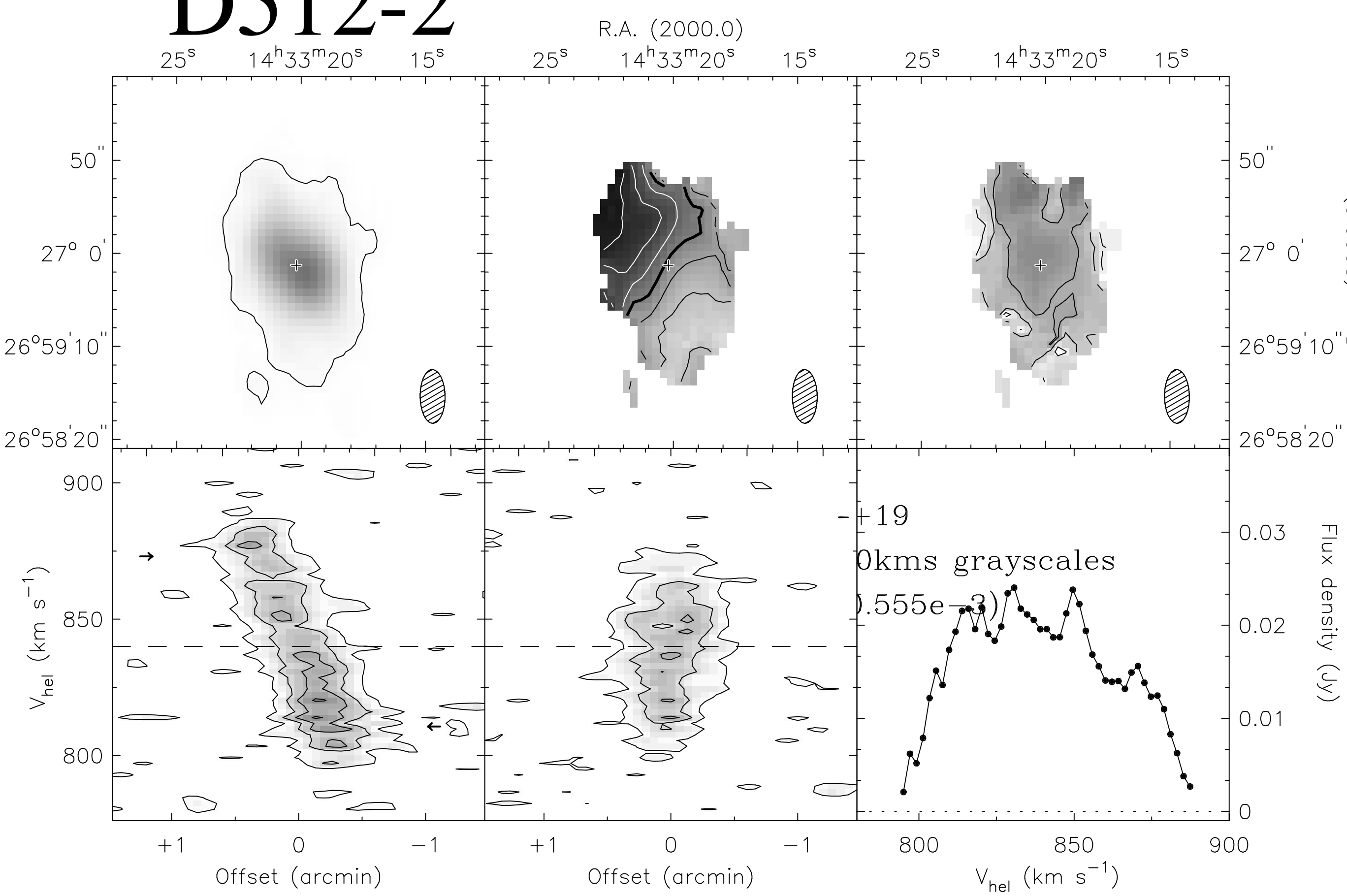

D575-2

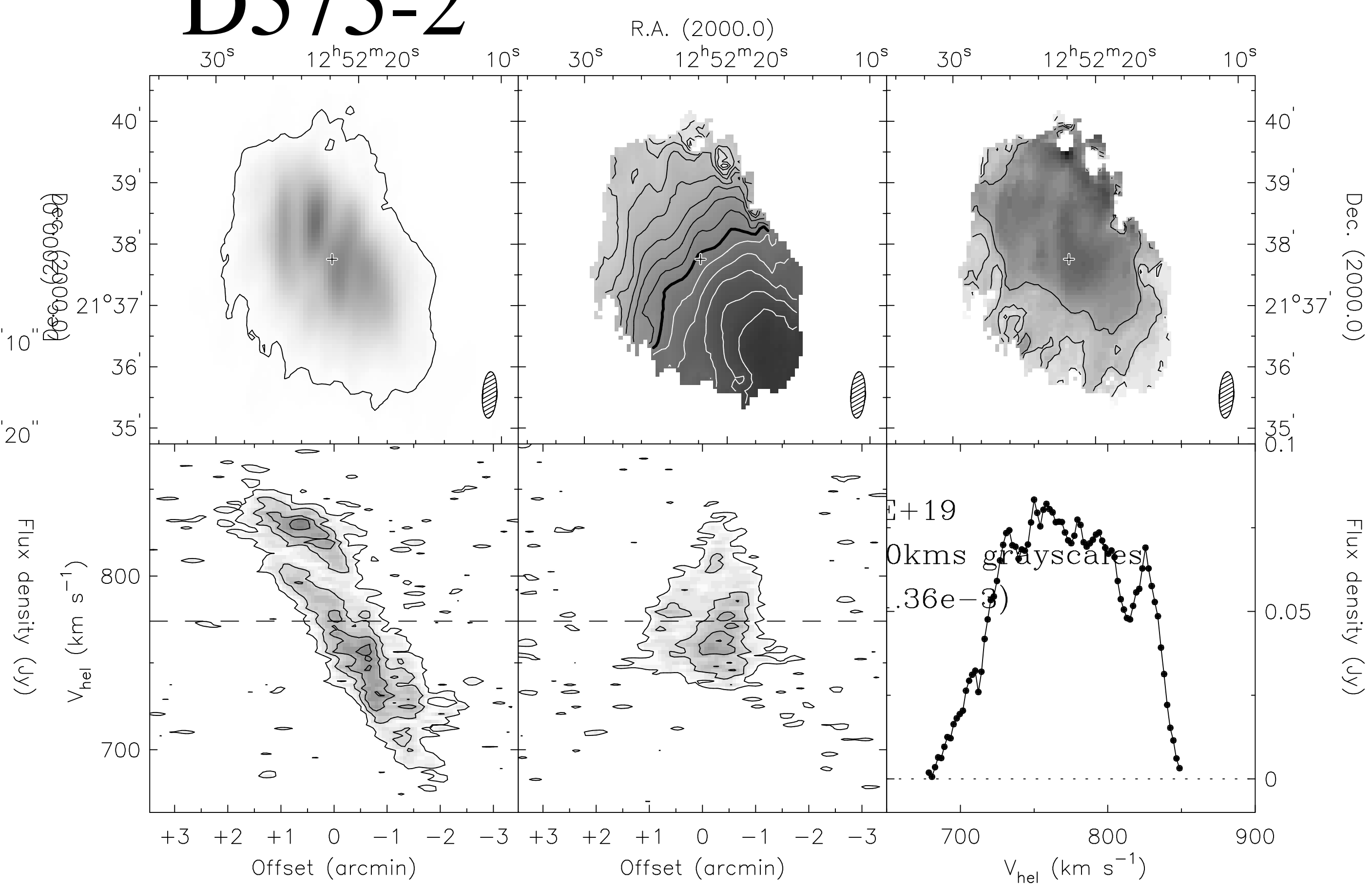

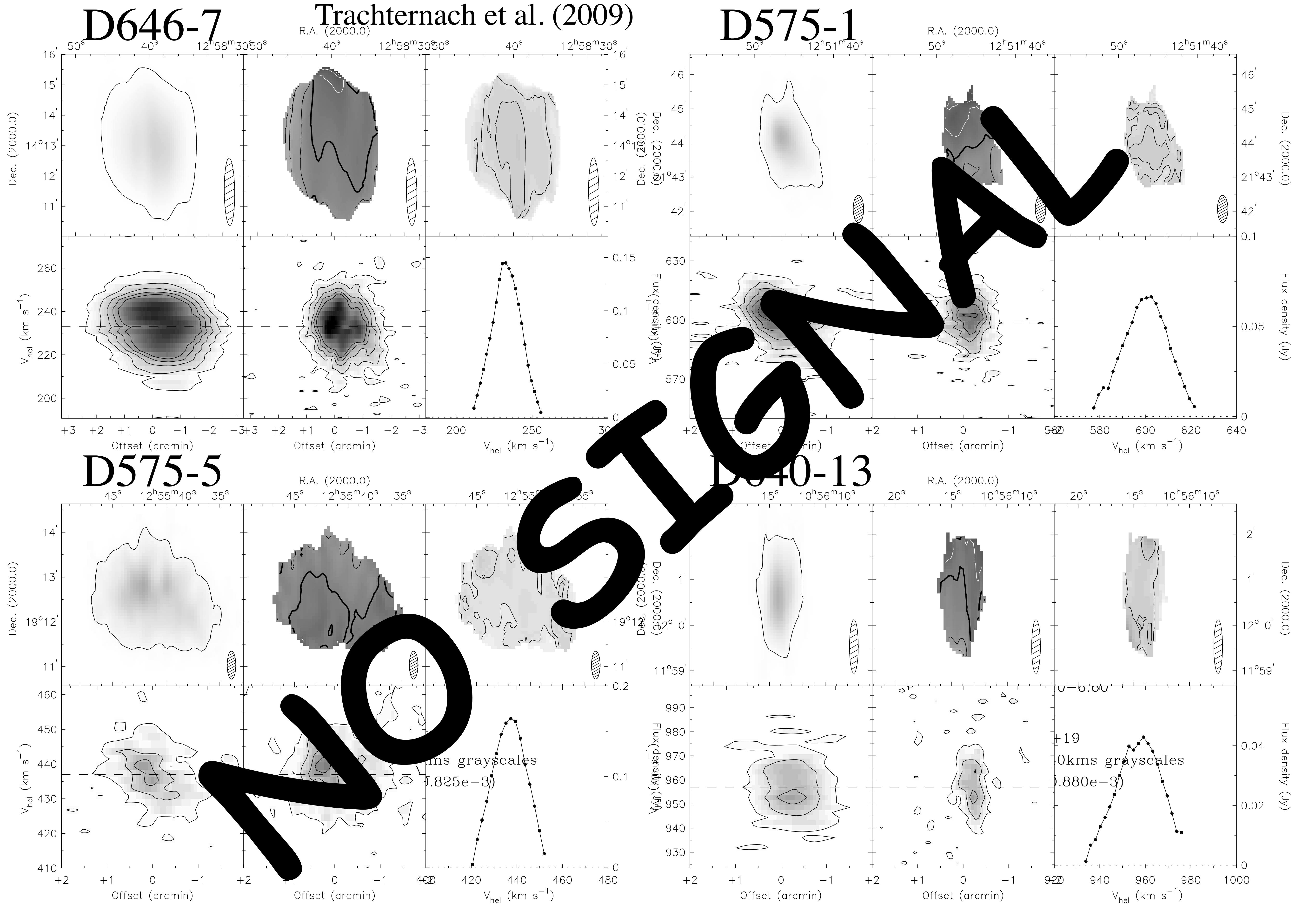

Note that you can measure a line-width even if there is no evidence of rotation.

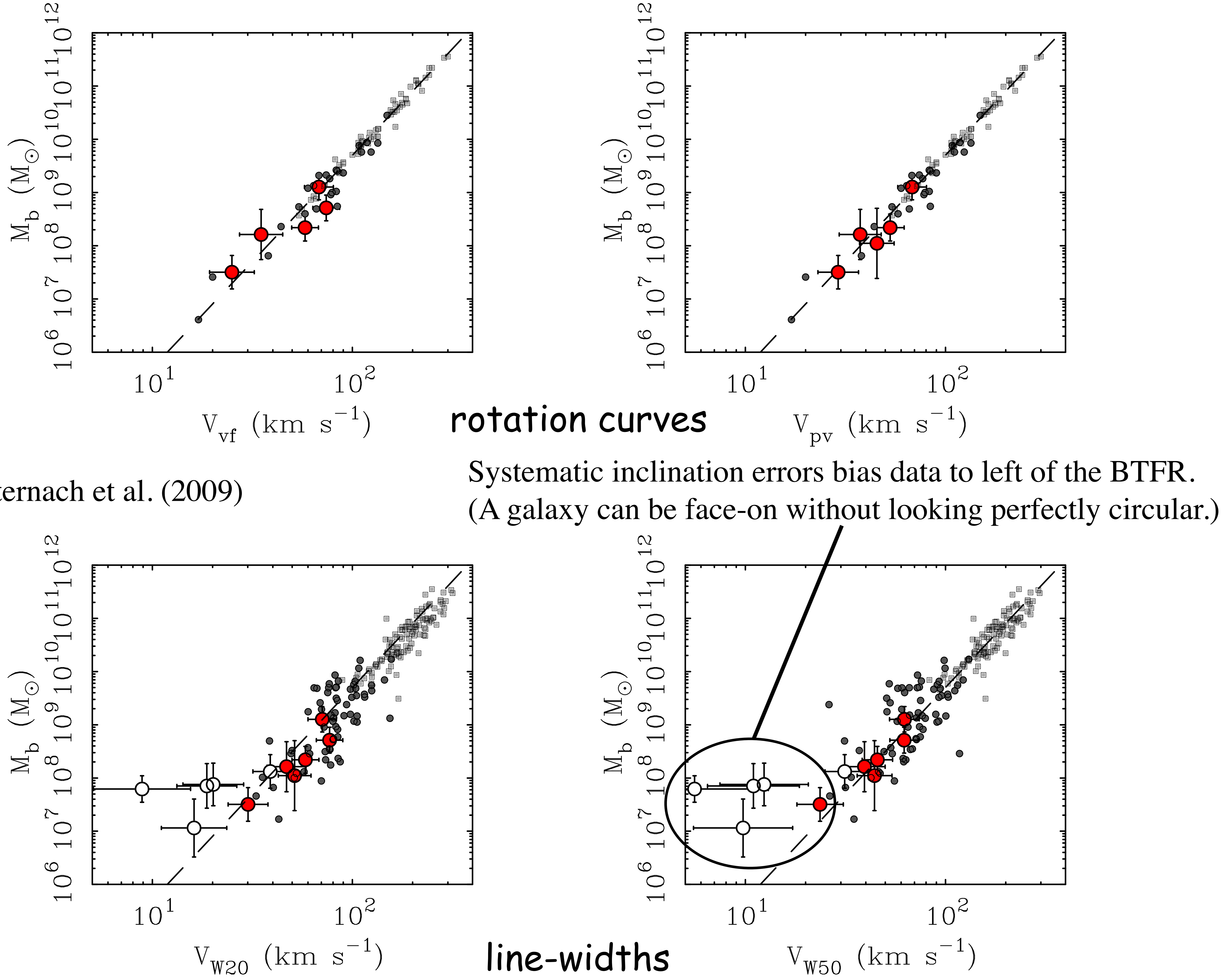
M_b ($M_\odot$)
10^6 10^7 10^8 10^9 10^{10} 10^{11} 10^{12}
10^1 10^2
V_{vf} (km s^{-1})
rotation curves
V_{pv} (km s^{-1})
Systematic inclination errors bias data to left of the BTFR.
(A galaxy can be face-on without looking perfectly circular.)
Trachternach et al. (2009)
V_{W20} (km s^{-1})
line-widths
V_{W50} (km s^{-1})

Stellar Mass Tully-Fisher relation

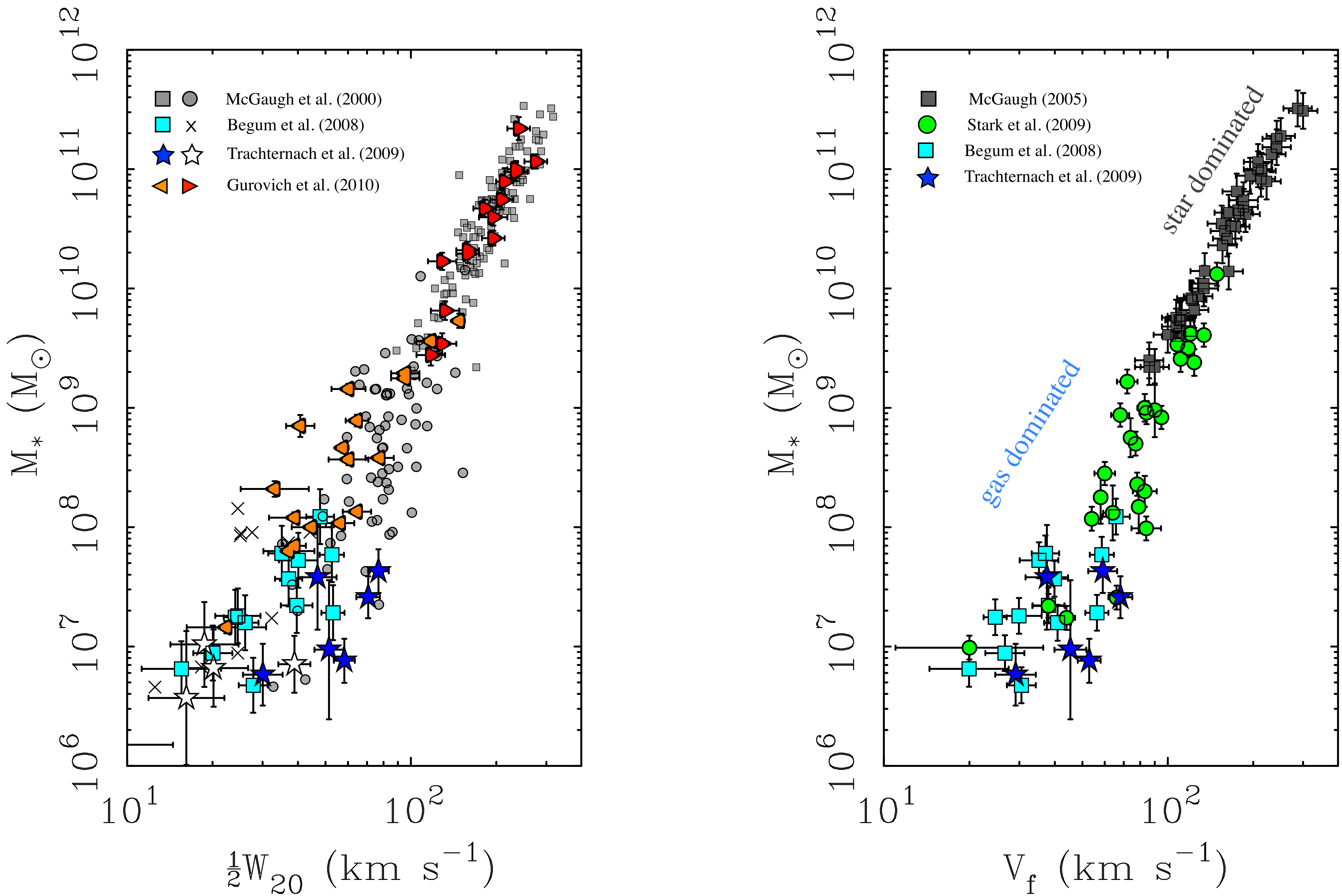

line-width

outer (flat) velocity

HI Tully-Fisher relation

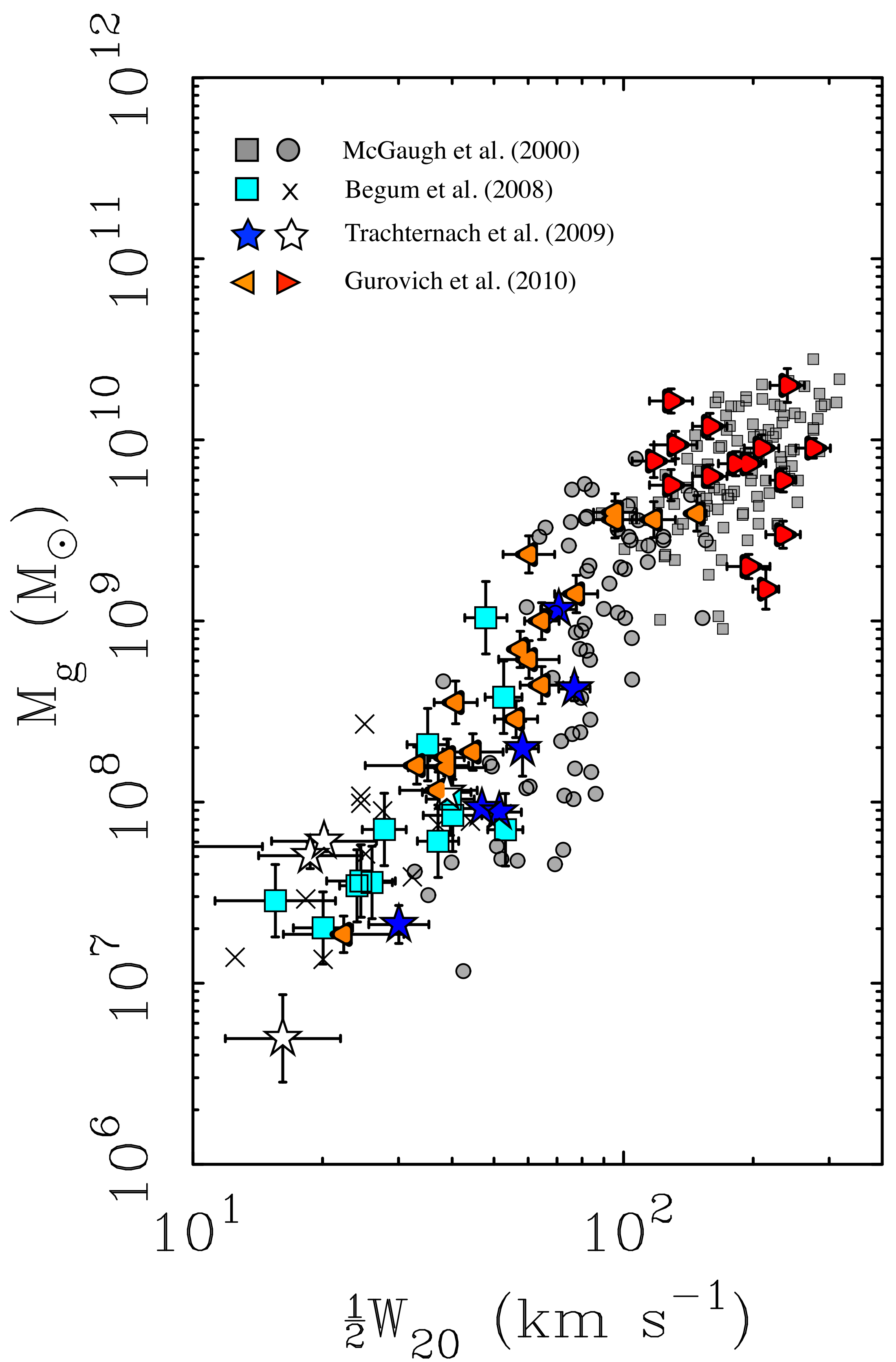

line-width

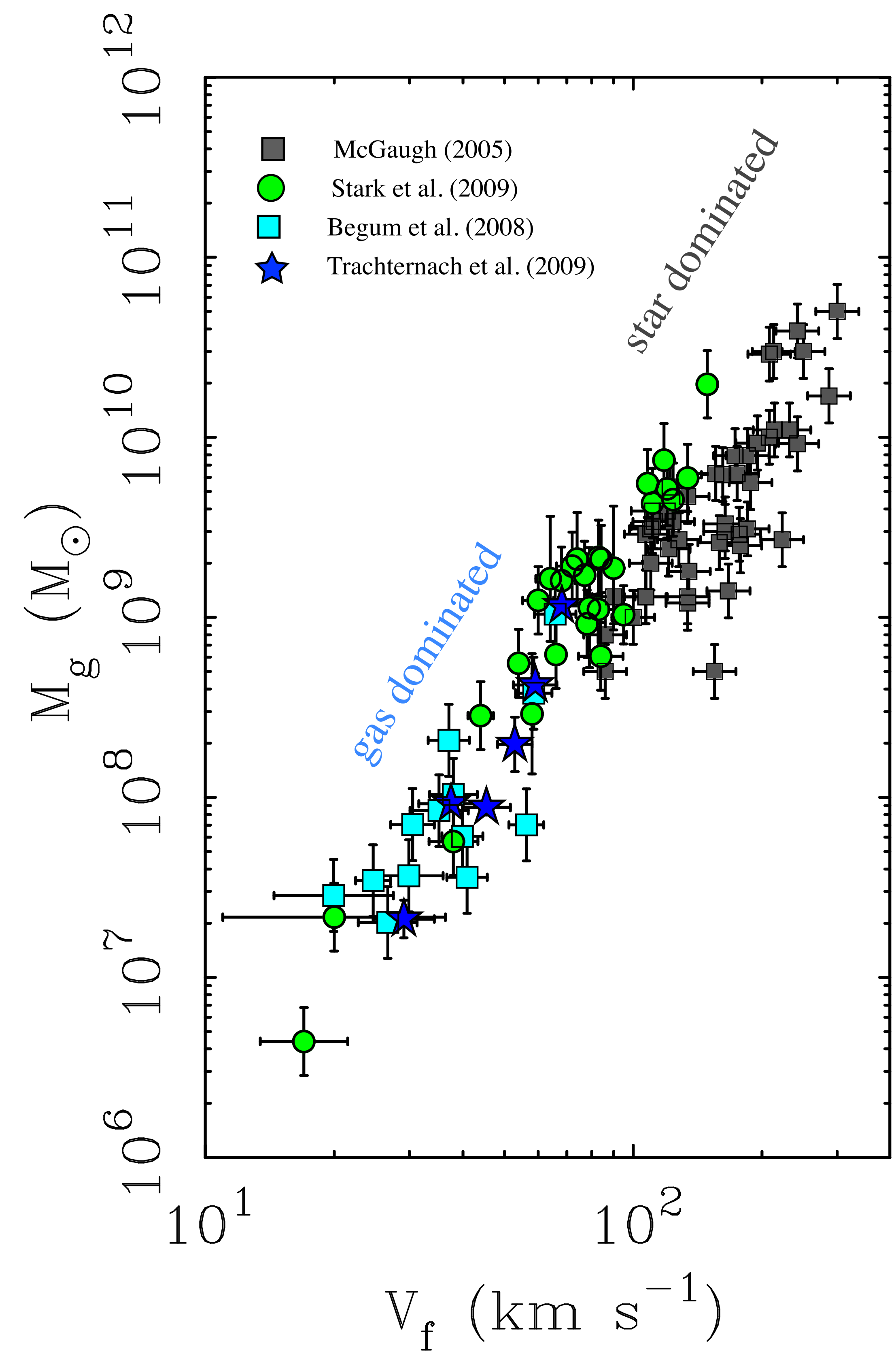

outer (flat) velocity

Baryonic Tully-Fisher relation: slope & scatter depend on Velocity estimator

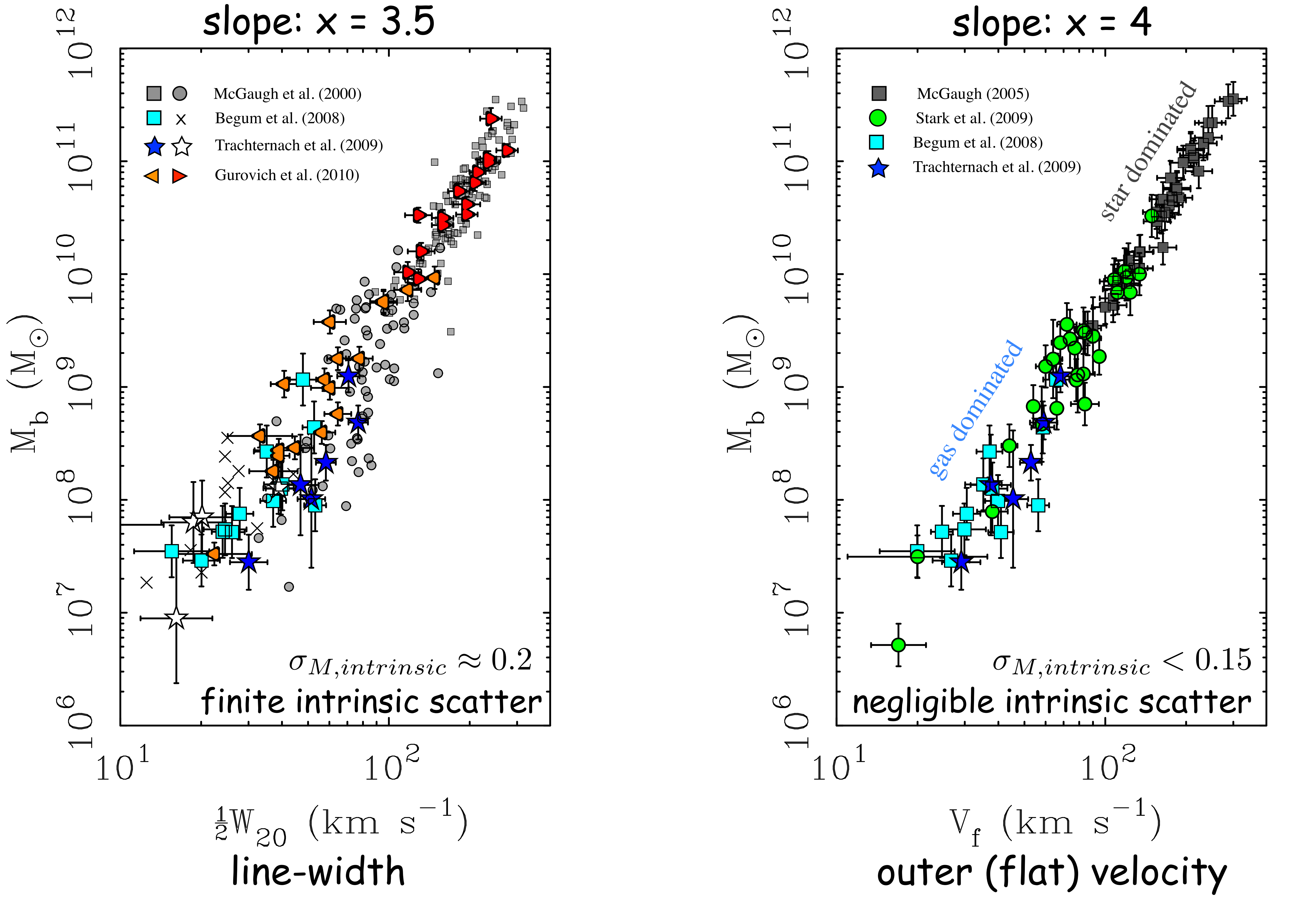

Gas dominated galaxies can provide absolute calibration of mass scale.

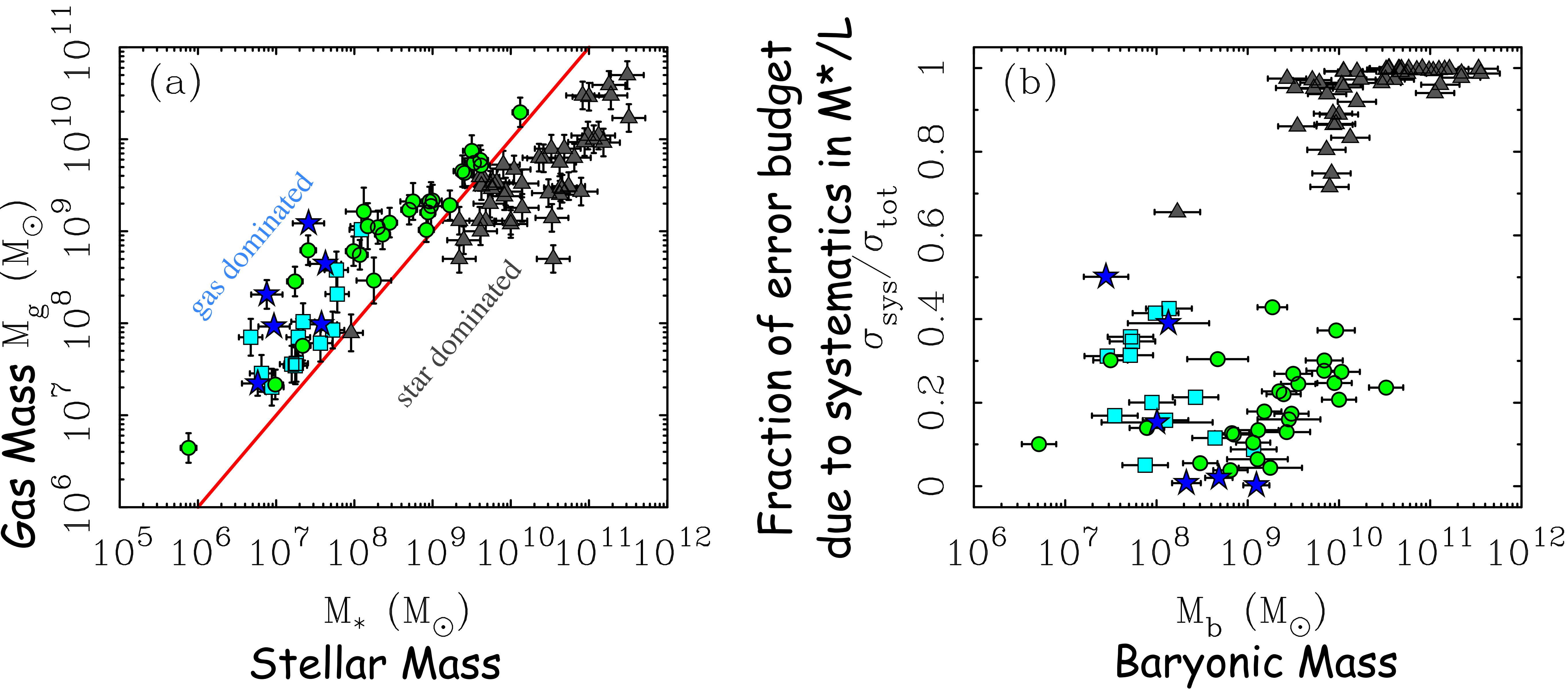

Systematic errors in M*/L no longer dominate the error budget for galaxies with Mg > M*.

Gas Rich Galaxy Baryonic Tully-Fisher relation
(Stark et al 2009; Trachternach et al 2009; McGaugh 2011, 2012)

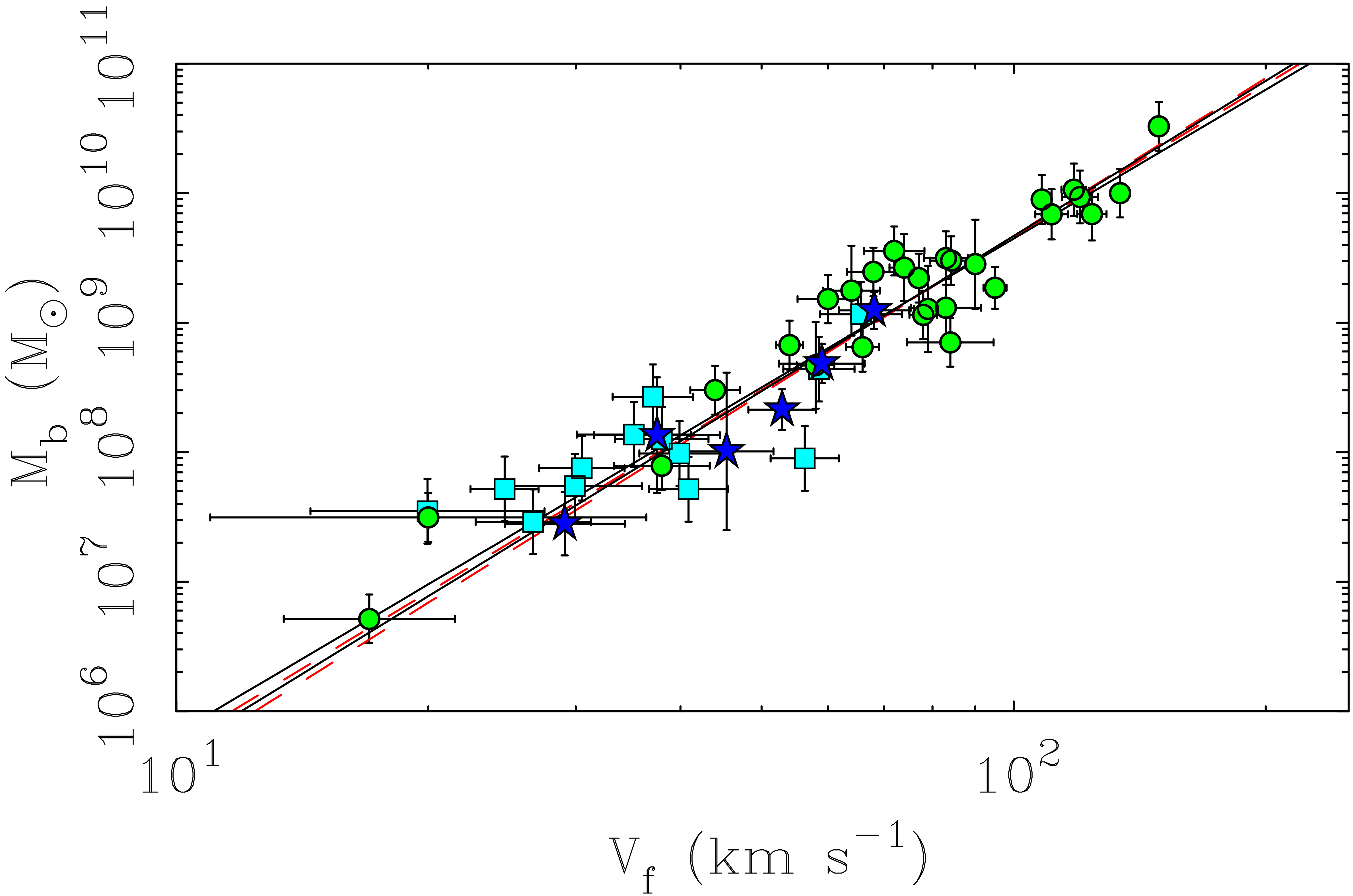

select $M_g > M_\star$

try fits with many different combinations
of IMF and populations synthesis models

Table 4. BTF Fit to Gas Dominated Galaxies

$M_b = A\, V_f^x$

Subsample	N	$x_{v\|M}$	$A_{v\|M}$	$\chi^2_{\nu,v\|M}$	$x_{M\|v}$	$A_{M\|v}$	$\chi^2_{\nu,M\|v}$	x_{bis}	A_{bis}
Portinari-Kroupa	23	3.77	2.08	1.28	4.11	1.43	1.18	3.93	1.78
Portinari-Salpeter	14	3.59	2.44	1.42	4.37	1.02	1.46	3.94	1.79
Portinari-Kennicutt	26	3.74	2.14	2.01	4.33	0.99	1.85	4.01	1.62
Bell-Scaled Salpeter	23	3.77	2.09	1.41	4.09	1.47	1.31	3.93	1.80
Bell-Kroupa	26	3.72	2.17	2.30	4.36	0.94	2.10	4.01	1.61
Bell-Bottema	36	3.55	2.45	2.02	3.96	1.63	2.06	3.74	2.06

$$\text{slope } x = 3.94 \pm 0.07 \text{ (random)} \pm 0.08 \text{ (systematic)}$$

Stark, McGaugh, & Swaters (2009, AJ, 138, 392)

Fixing the slope to 4 gives $A = 47 \pm 6\ \mathrm{M_\odot\, km^{-4}\, s^4}$

Tully-Fisher

Provides a check on stellar mass-to-light ratios

Luminosity

Dashed line: fit to data
Solid Gray line: $M_b = 47 V_f^4$

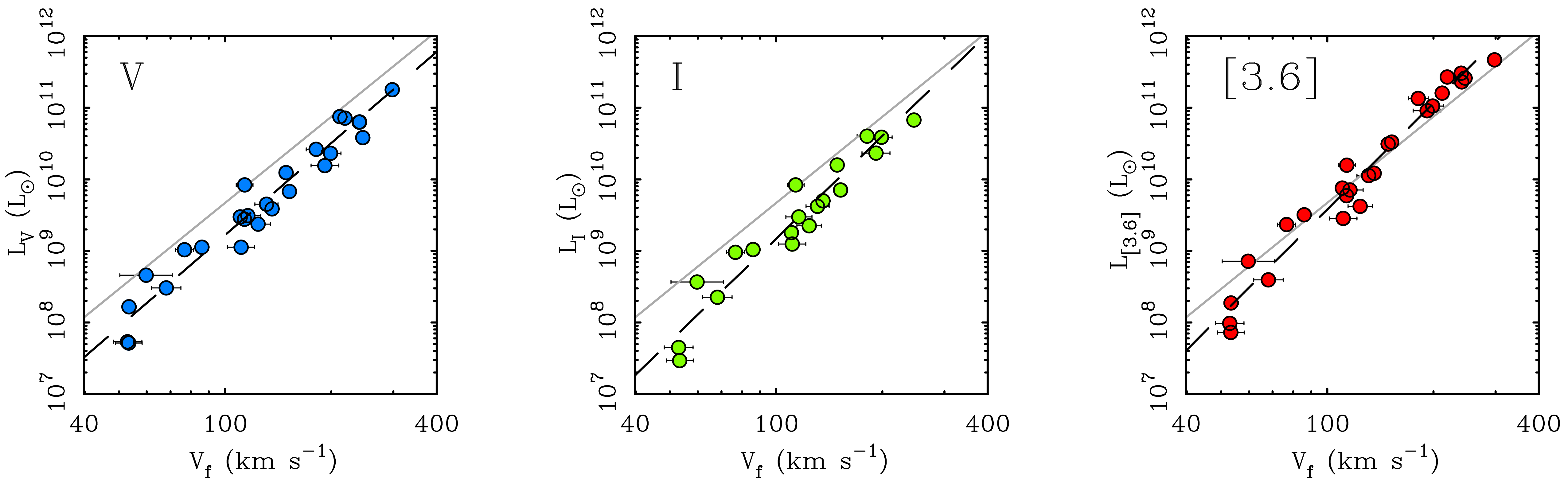

flat rotation speed

Tully-Fisher

Provides a check on stellar mass-to-light ratios

Stellar mass $M_* = \Upsilon_*^i L_i$

Dashed line: fit to data
Solid Gray line: $M_b = 47 V_f^4$

$\log \Upsilon_*^V = 1.3(B-V) - 0.63$ $\log \Upsilon_*^I = 0.6(B-V) - 0.28$ $\log \Upsilon_*^{[3.6]} = 0.5\ M_\odot / L_\odot$

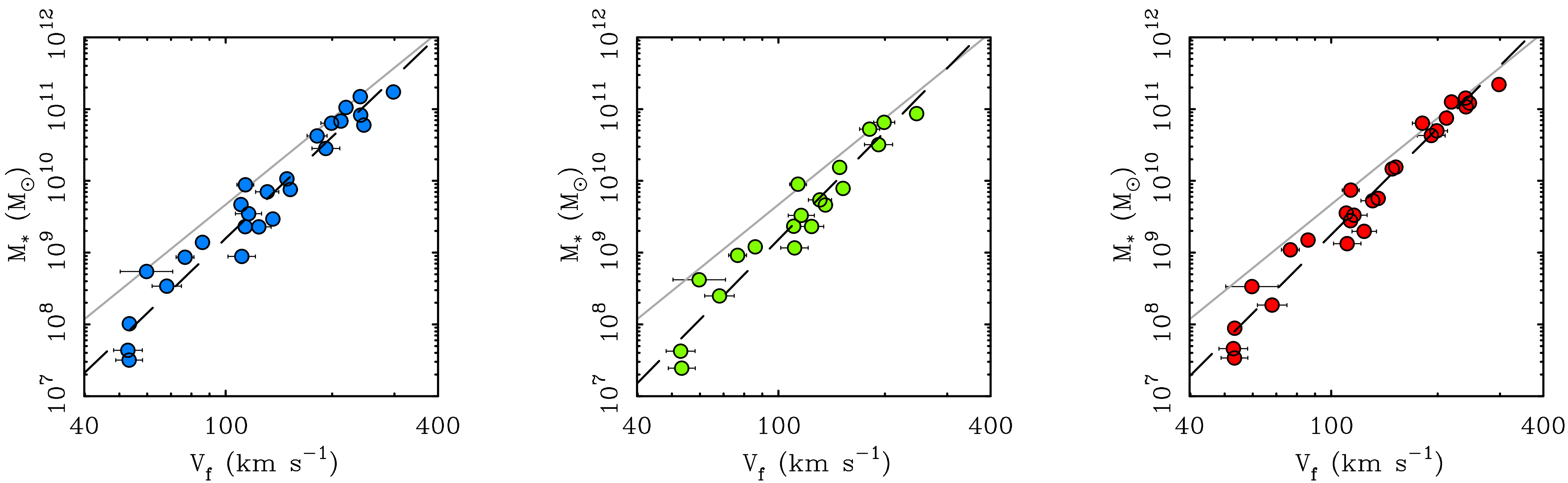

flat rotation speed

The stellar mass-to-light ratio depends on strongly on color in V, a bit in I, but is effectively constant at [3.6]

Tully-Fisher

Provides a check on stellar mass-to-light ratios

Baryonic mass

Dashed line: fit to data
Solid Gray line: $M_b = 47V_f^4$

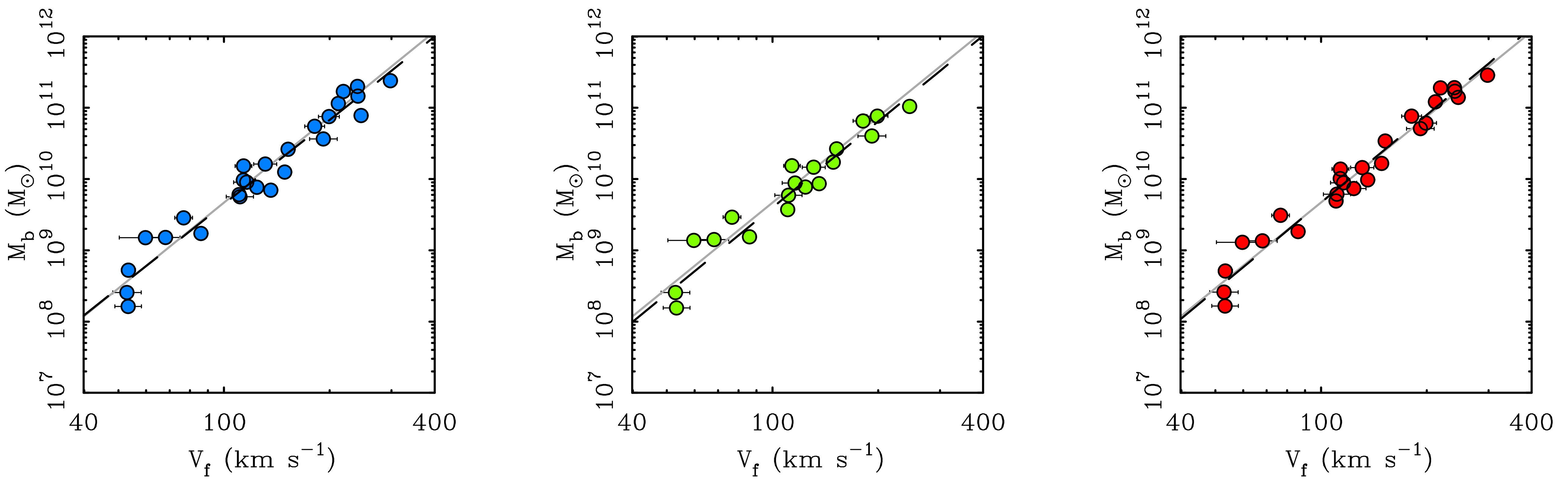

flat rotation speed

2019 data:
arXiv:1909.02011

Blue: Distances known to better than 20%
Gray: Distances known to worse than 20%
Red: Milky Way

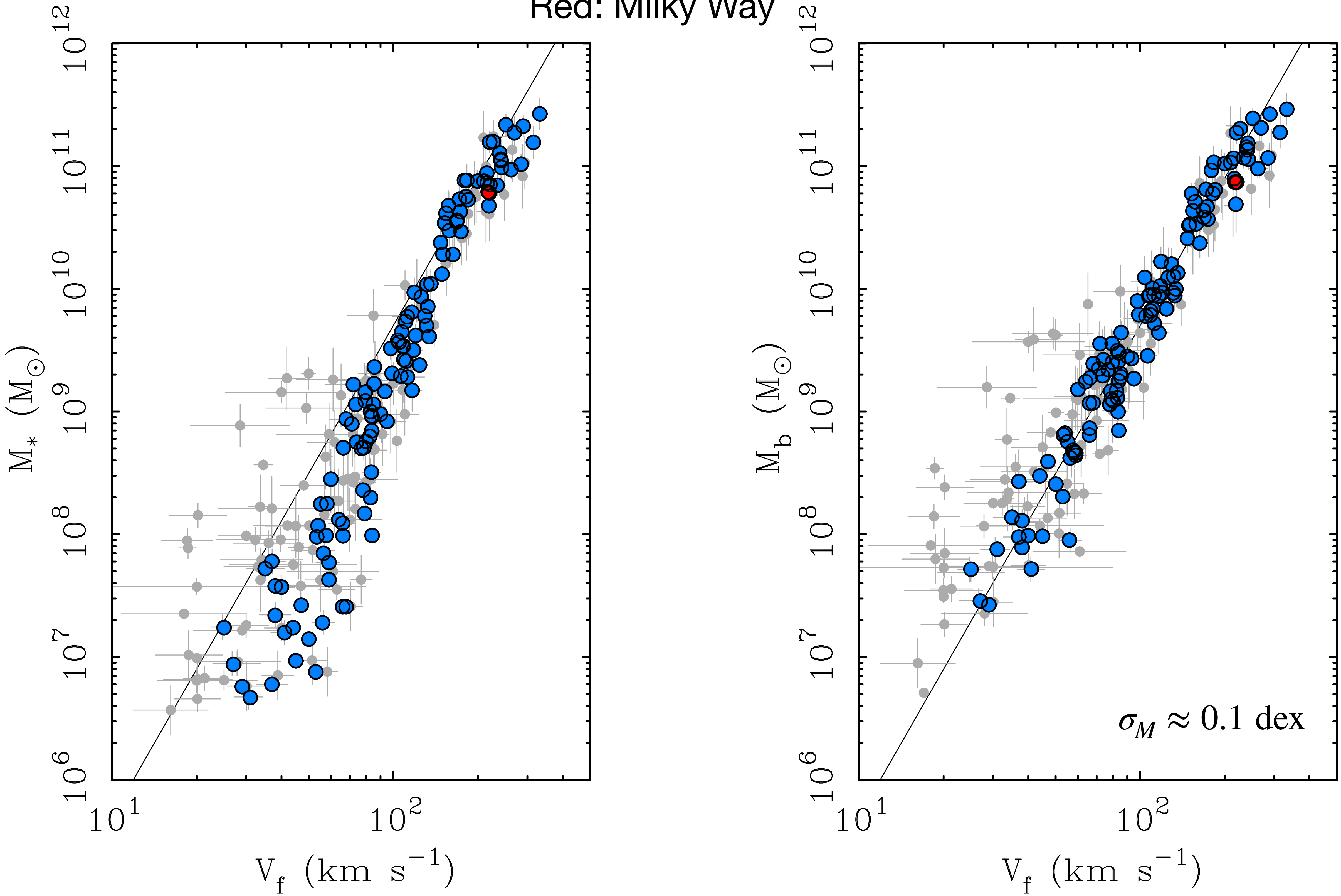

Intrinsic scatter small
(Lelli et al 2016, 2019)

No residuals from TF with size or surface density

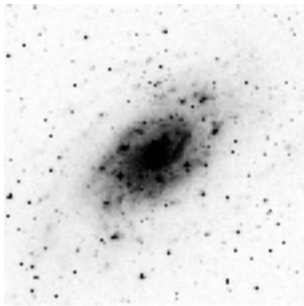

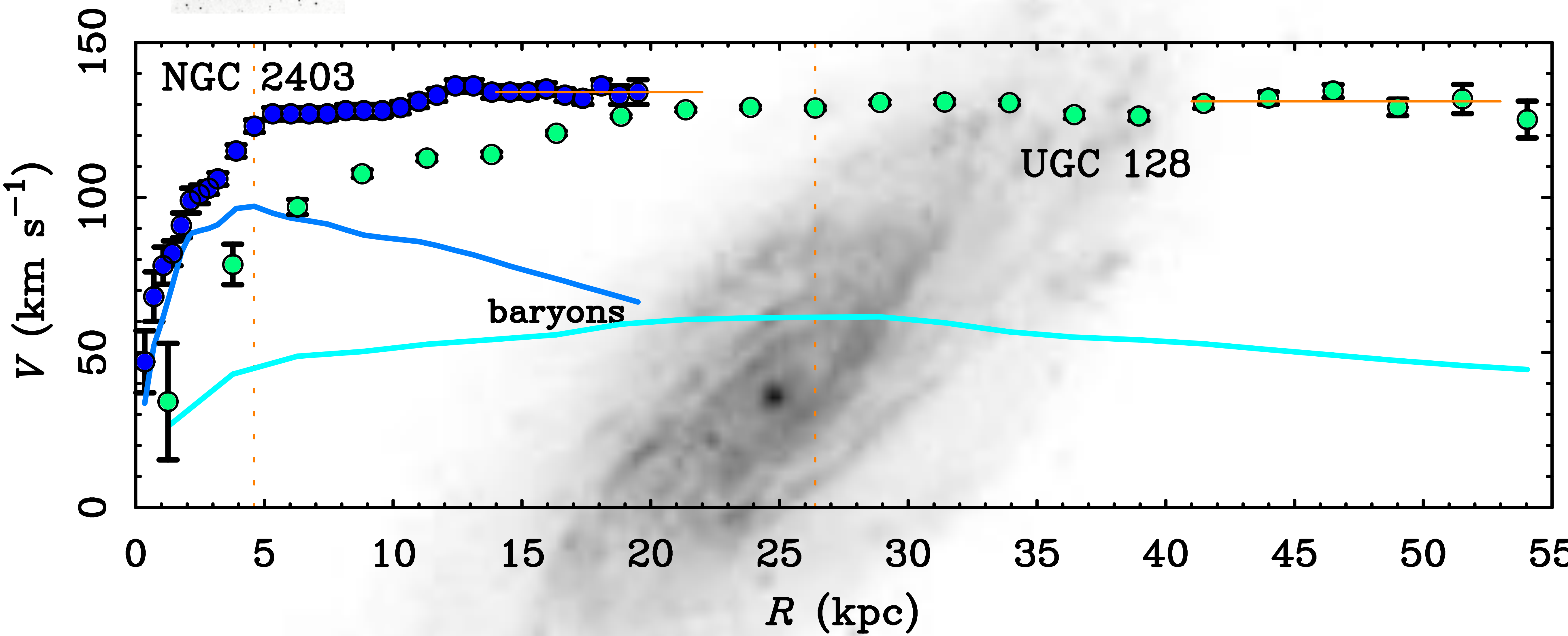

Same (M,V) but very different size and surface density

which is strange, since $V^2 = \frac{GM}{R}$

No residuals from TF with size or surface brightness

(Zwaan et al 1995; Sprayberry et al 1995; McGaugh & de Blok 1998)

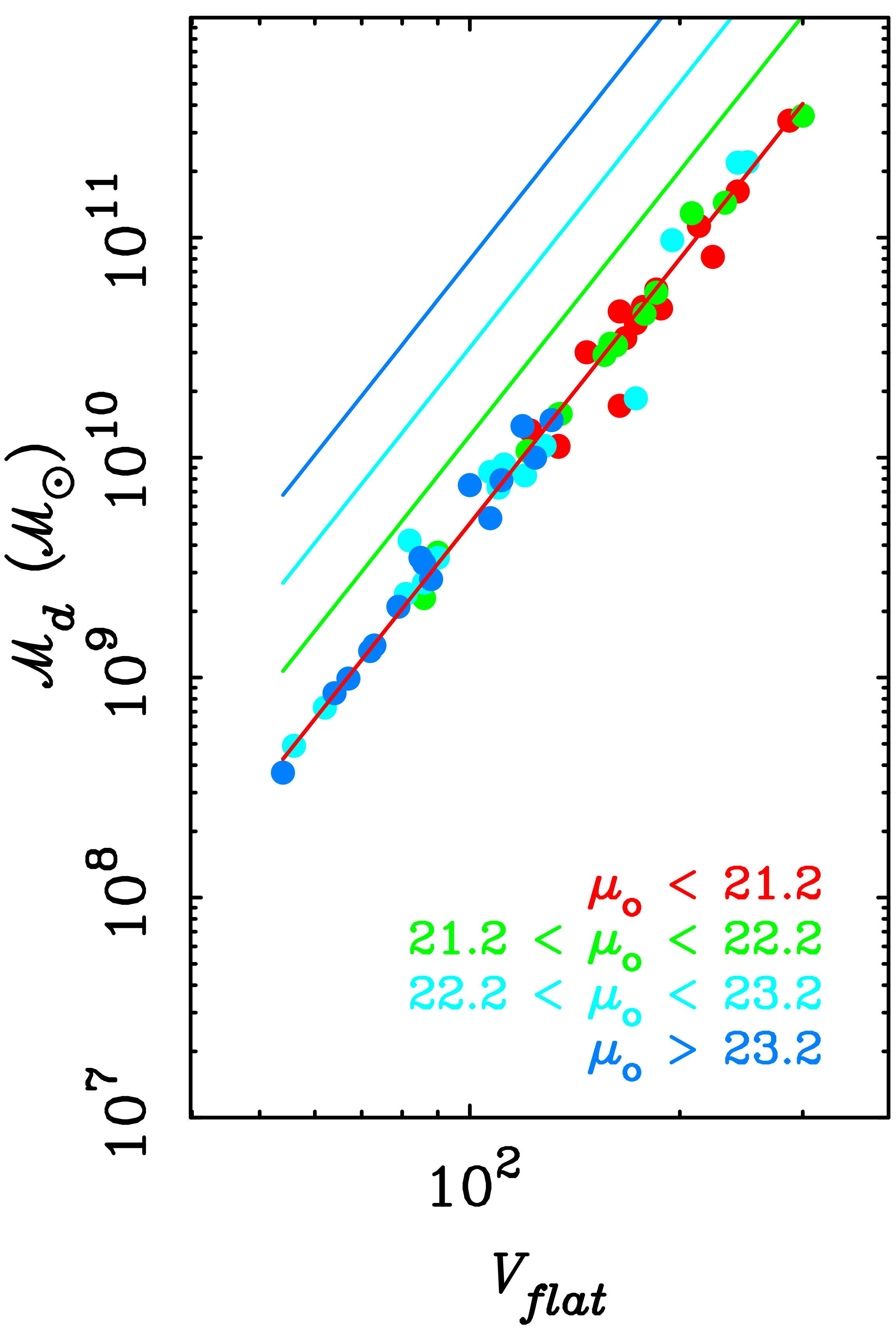

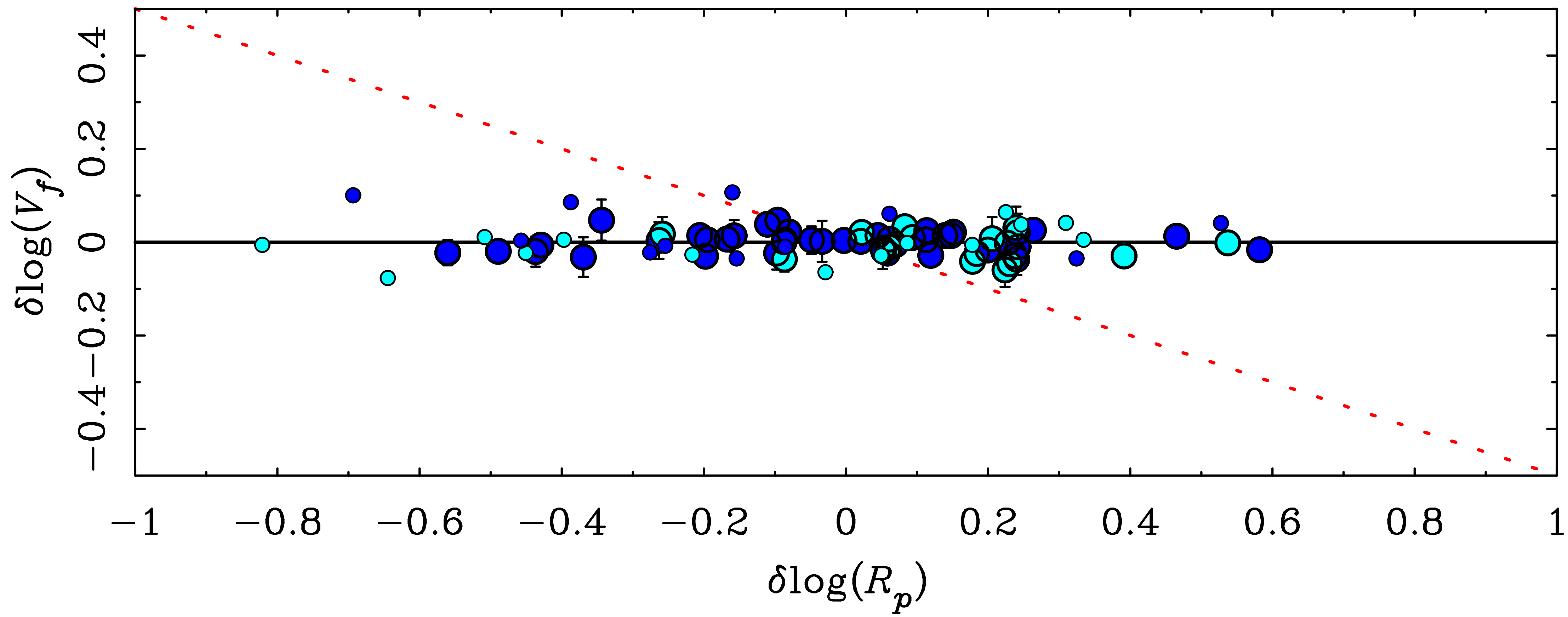

No residuals from TF with size or surface density for disks

$$V^2 = \frac{GM}{R} \rightarrow \frac{\delta \log(V)}{\delta \log(R)} = -\frac{1}{2}$$ expected slope (dotted line)

Note: large range in size at a given mass or velocity

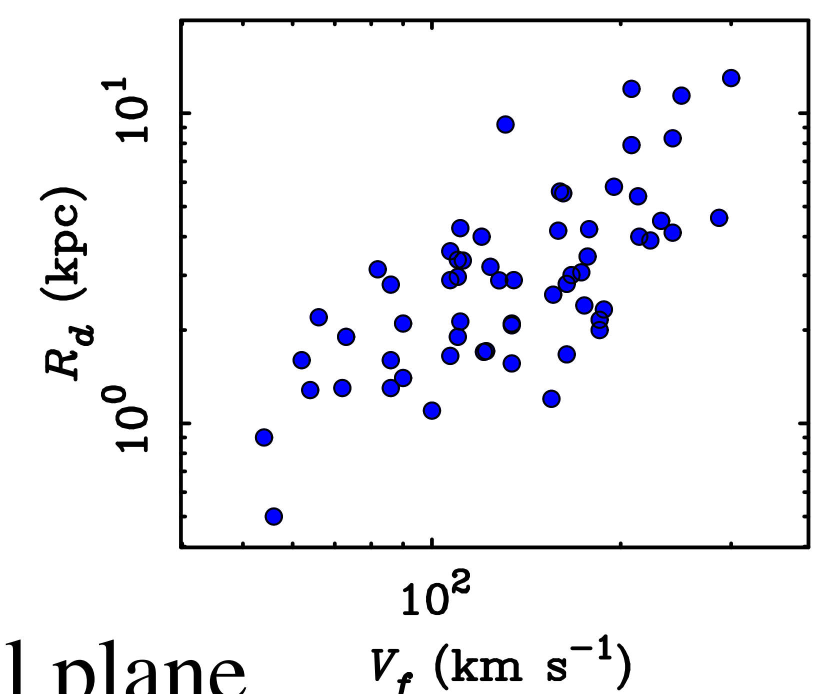

TF already edge-on projection of disk fundamental plane

Baryonic TF Relation

- Fundamentally a relation between the baryonic mass of a galaxy and its rotation velocity
  - $M_b = M_* + M_g = 47 V_f^4$ (McGaugh 2012)
  - doesn't matter if it is stars or gas
- Intrinsic scatter negligibly small
  - Can mostly be accounted for by the expected variation in stellar M*/L
- Physical basis of the relation remains unclear

Relation has real physical units if slope has integer value - Slope appears to be 4 *if* Vflat is used.

Rotation curve amplitude depends on the mass of stars and gas (BTFR)

Rotation curve shape depends on the distribution of stars and gas

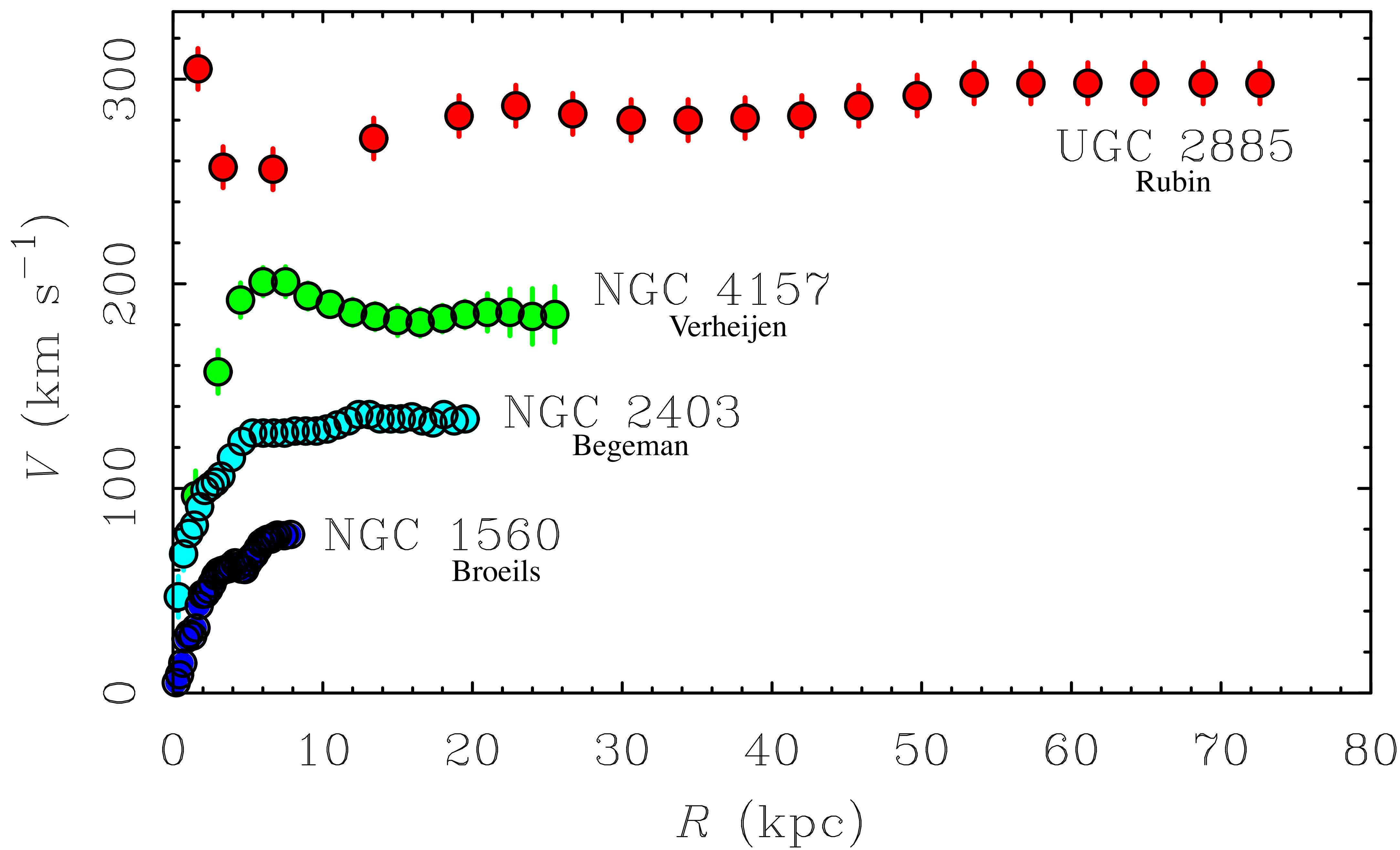

only near the limits of the optical image ($\kappa \approx 1$); velocities of highest-luminosity Sc's reach 100 km s^{-1} in less than 1% of the optical radius ($\kappa < 0.01$). The plot of log κ versus log V_{max} (Fig. 3) emphasizes that κ is a reliable estimator of V_{max} and, hence, of absolute magnitude. Ignoring resolution effects for the most distant galaxies, this diagram is distance independent. Furthermore, a comparison of Figures 1 and 2 shows that the (log κ, M_B) relation is similar in form and scatter to the (log V_{max}, M_B) relation, i.e., the conventional TF relation. The choice of 100 km s^{-1} as a fiducial mark in measuring κ is not particularly critical to the success of the (log κ, M_B) relation, although it should be located beyond local nuclear effects so as to relate to the overall rotation curve. It should not be affected by nonaxisymmetric barlike motions and local velocity perturbations often observed at small nuclear distances.

From our published rotation curves, it is clear that an adopted measure could be chosen from a fairly wide range of velocities up to and including, of course, the velocity peak. Any one of such measures would serve as a luminosity discriminant. Thus the relationships exhibited in Figures 1 and 2 are representative of a family of dynamical-luminosity relationships. The family of such measures will be explored in detail in a future paper.

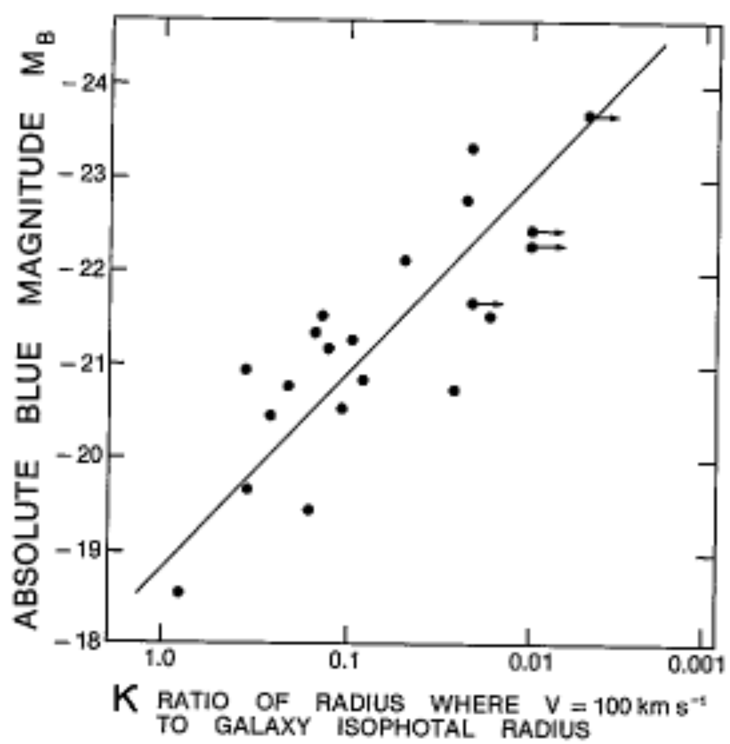

FIG. 2.—The correlation of M_B with log κ, the radial distance in the galaxy where the rotational velocity equals 100 km s^{-1}, in units of the isophotal radius. For lowest-luminosity Sc galaxies, the rotational velocity reaches 100 km s^{-1} only near the limits of the optical image ($\kappa \approx 1$), while for high-luminosity Sc's, the rotational velocity reaches 100 km s^{-1} in less than 1% of the optical radius ($\kappa < 0.01$).

nical scale and in Figure 4b scaled to the size of the galaxy. At every radial distance r in the constant-

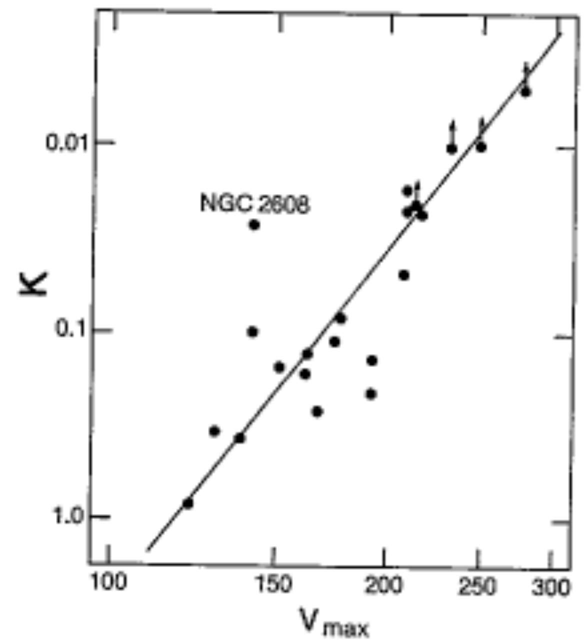

FIG. 3.—The correlation of log κ, the radius where the rotational velocity equals 100 km s^{-1} in units of the isophotal radius, vs. log V_{max}. The line is the mean of the two regressions and has a slope equal to 6.3 ± 0.5. NGC 2608, the only strongly barred galaxy in the sample, was excluded from the solution.

known for a long time

Rotation curve
shapes correlate
with galaxy properties

Rubin, Burstein, & Thonnard 1980, *ApJ*, **242**, L149

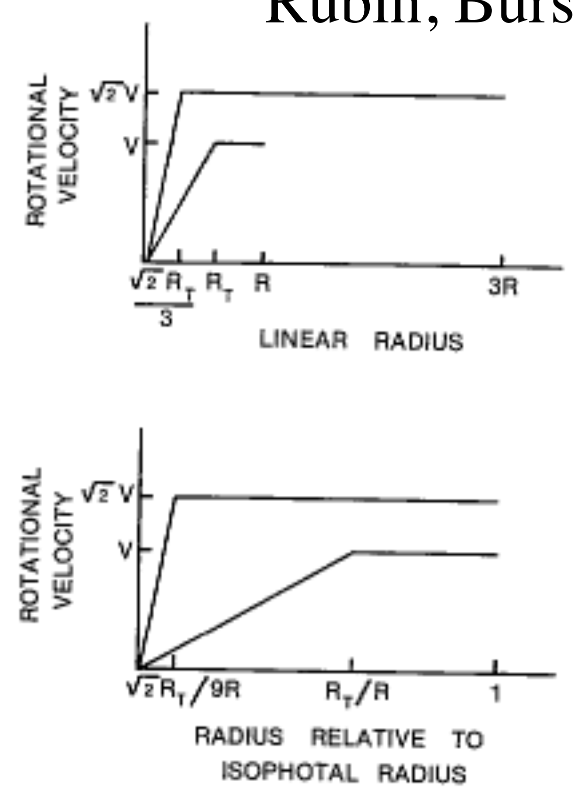

FIG. 4.—Schematic rotation curves for two Sc galaxies on a linear (*upper*) and relative (*lower*) radius scale. The higher-luminosity galaxy is chosen to have its velocity in the flat portion $\sqrt{(2)}$ times that of the lower-luminosity galaxy. Then the nuclear velocity gradient, turnover radius, and radial extent are fixed by the observations as shown (see text and Table 2).

Remember our TF pair?

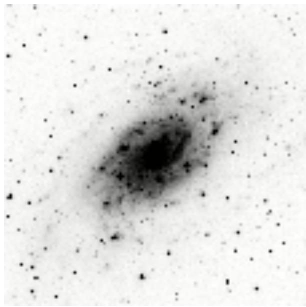

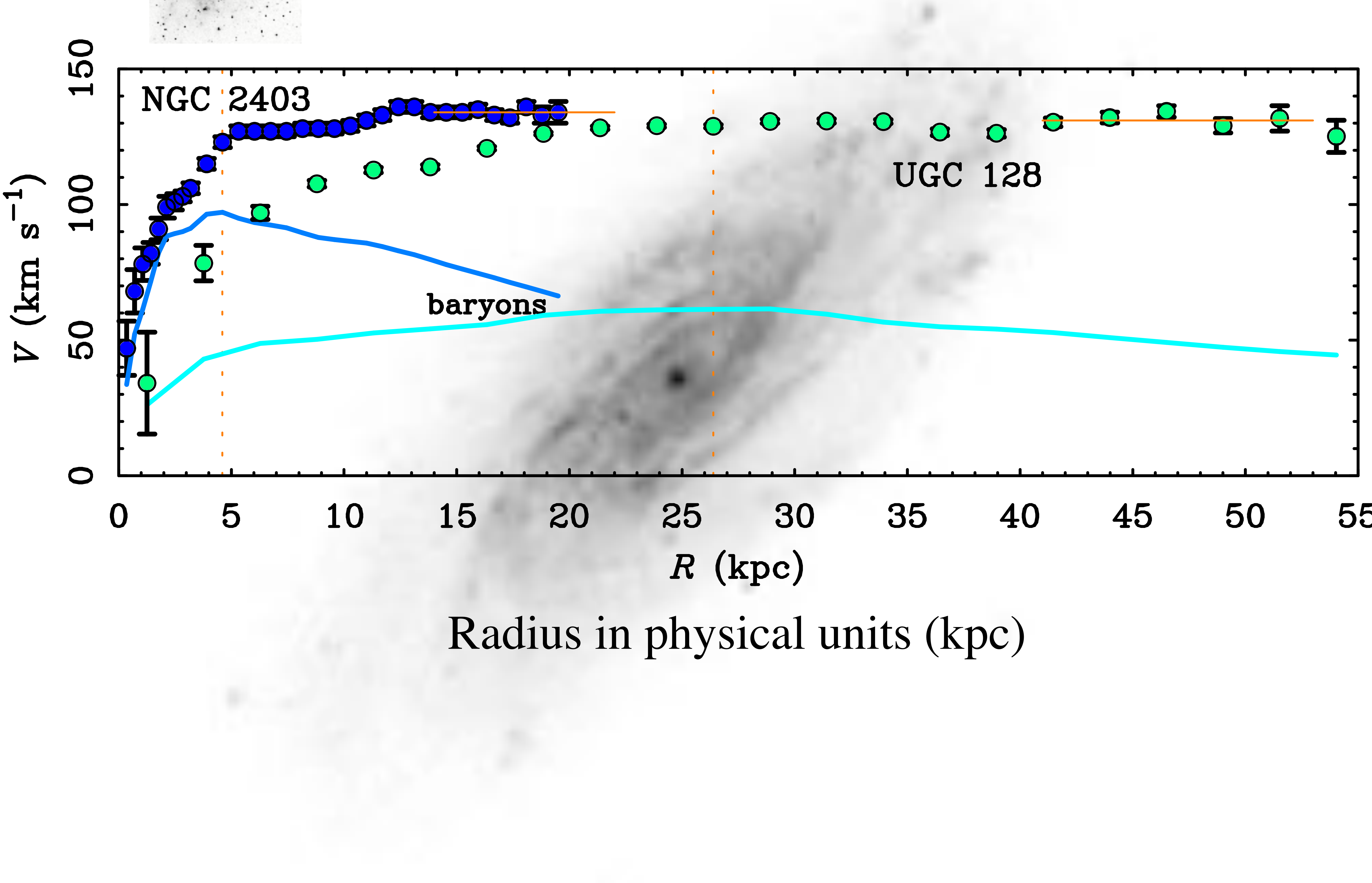

Radius in physical units (kpc)

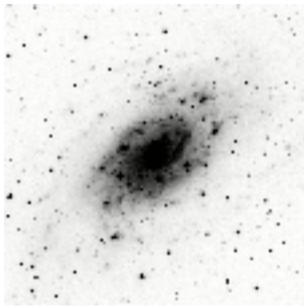

The dynamics knows about the distribution of baryons, not just their total mass

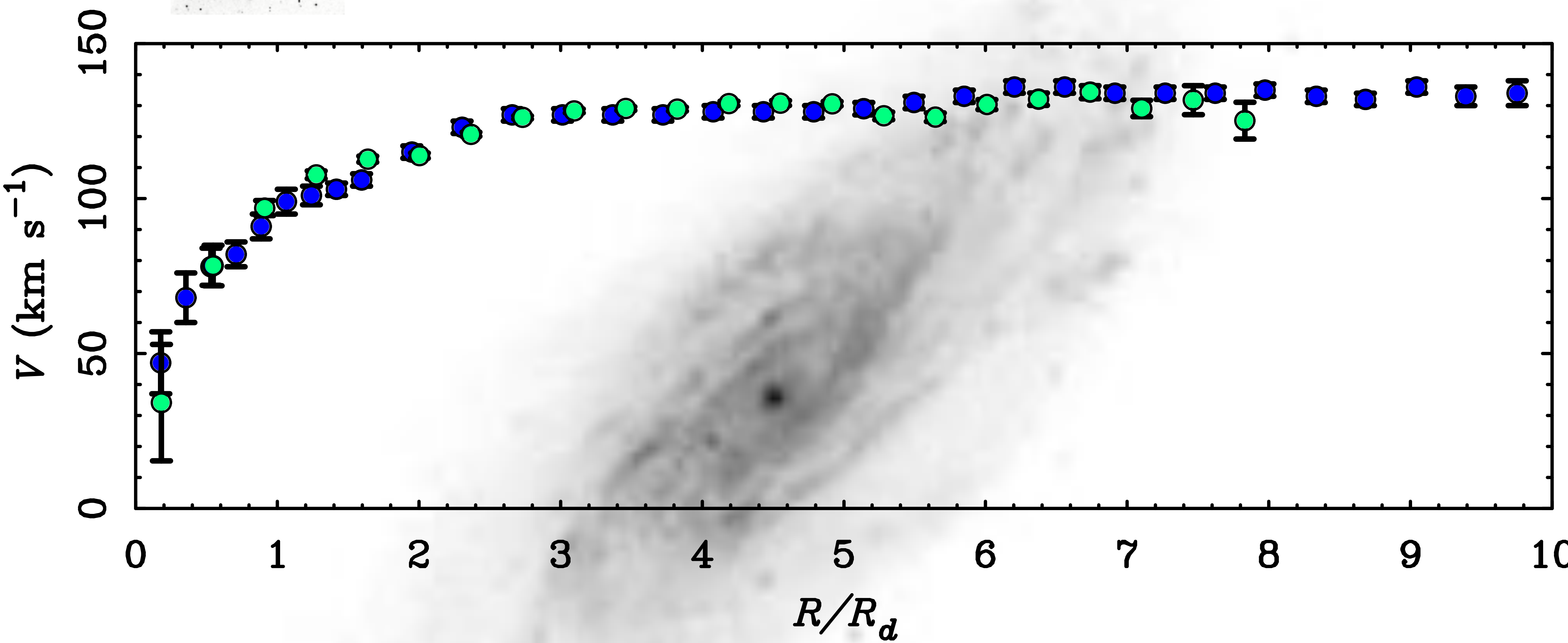

Radius normalized by size of disk.

Persic & Salucci 1996
de Blok & McGaugh 1996
Tully & Verheijen (1998)
Nordermeer & Verheijen (2007) [URC nor quite right formulation]
Swaters et al. (2009)

Rotation curve shape correlates with baryonic surface density

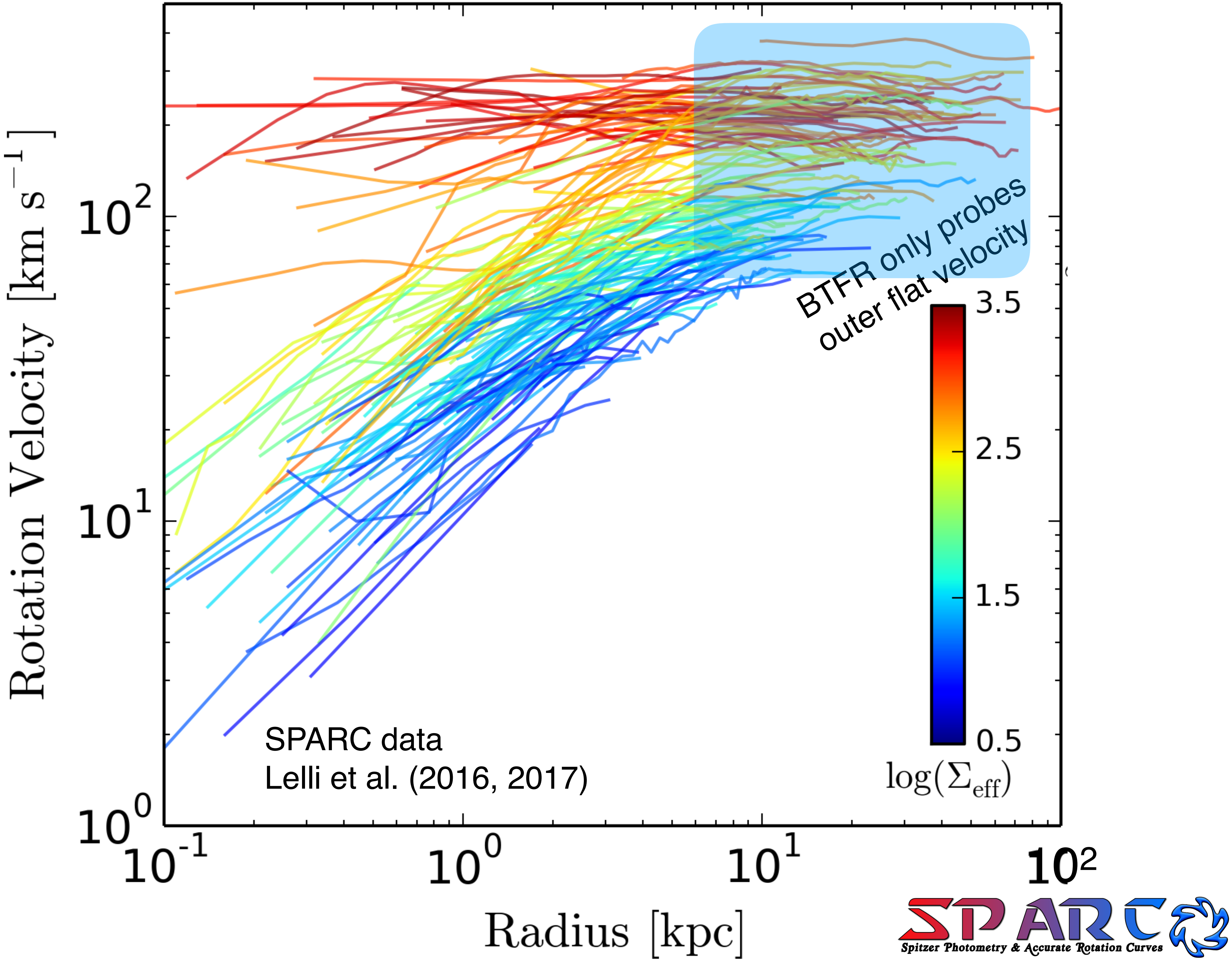

Rotation curve shape correlates with baryonic surface density

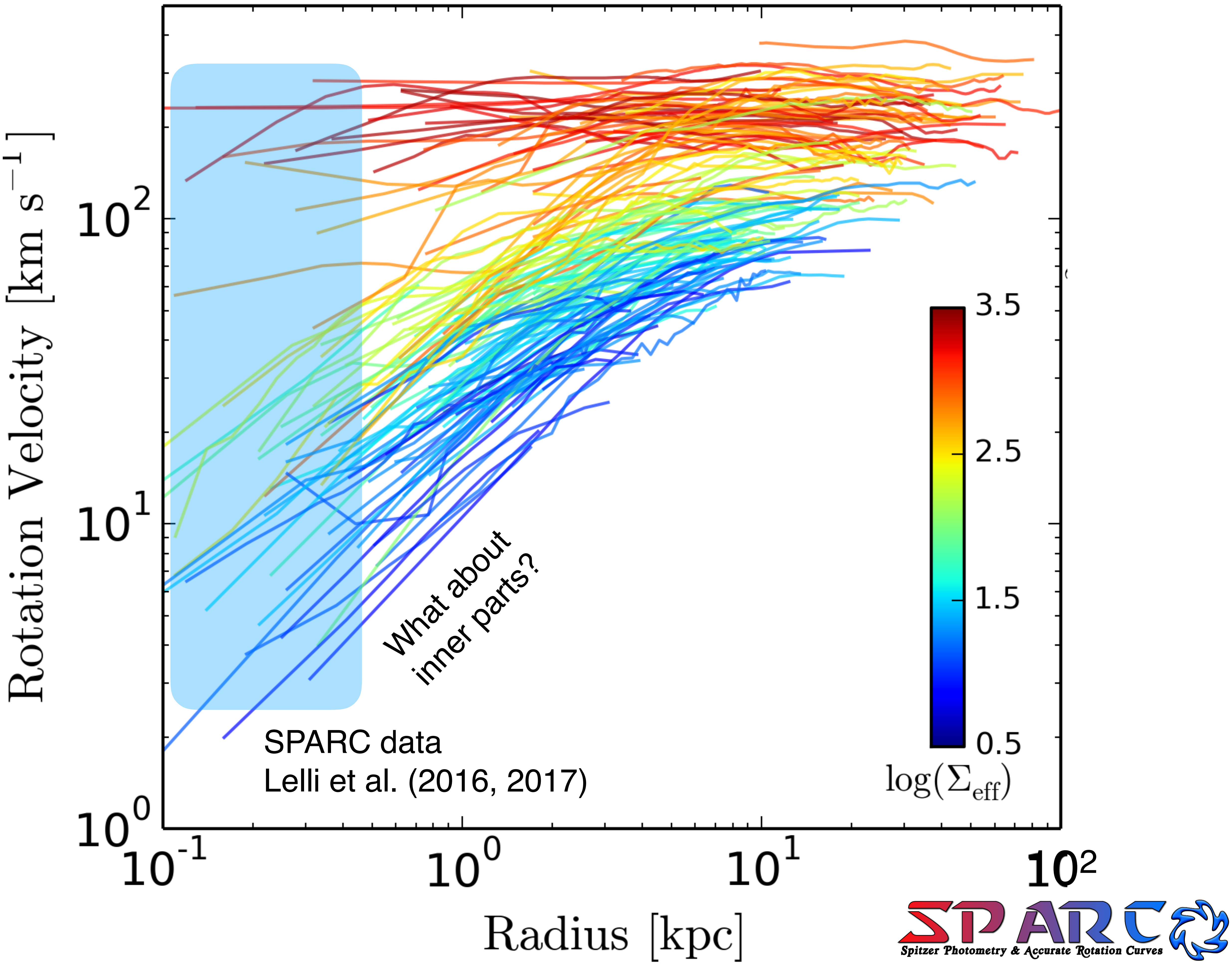

Central Density Relation

Lelli et al. (2016)

The *dynamical* central mass surface density correlates with the central surface brightness of stars in galaxies.

central dynamical surface density

Toomre (1963)

$$\Sigma_{dyn}(0) = \frac{1}{2\pi G}\int_0^\infty \frac{V^2(R)}{r^2}dR$$

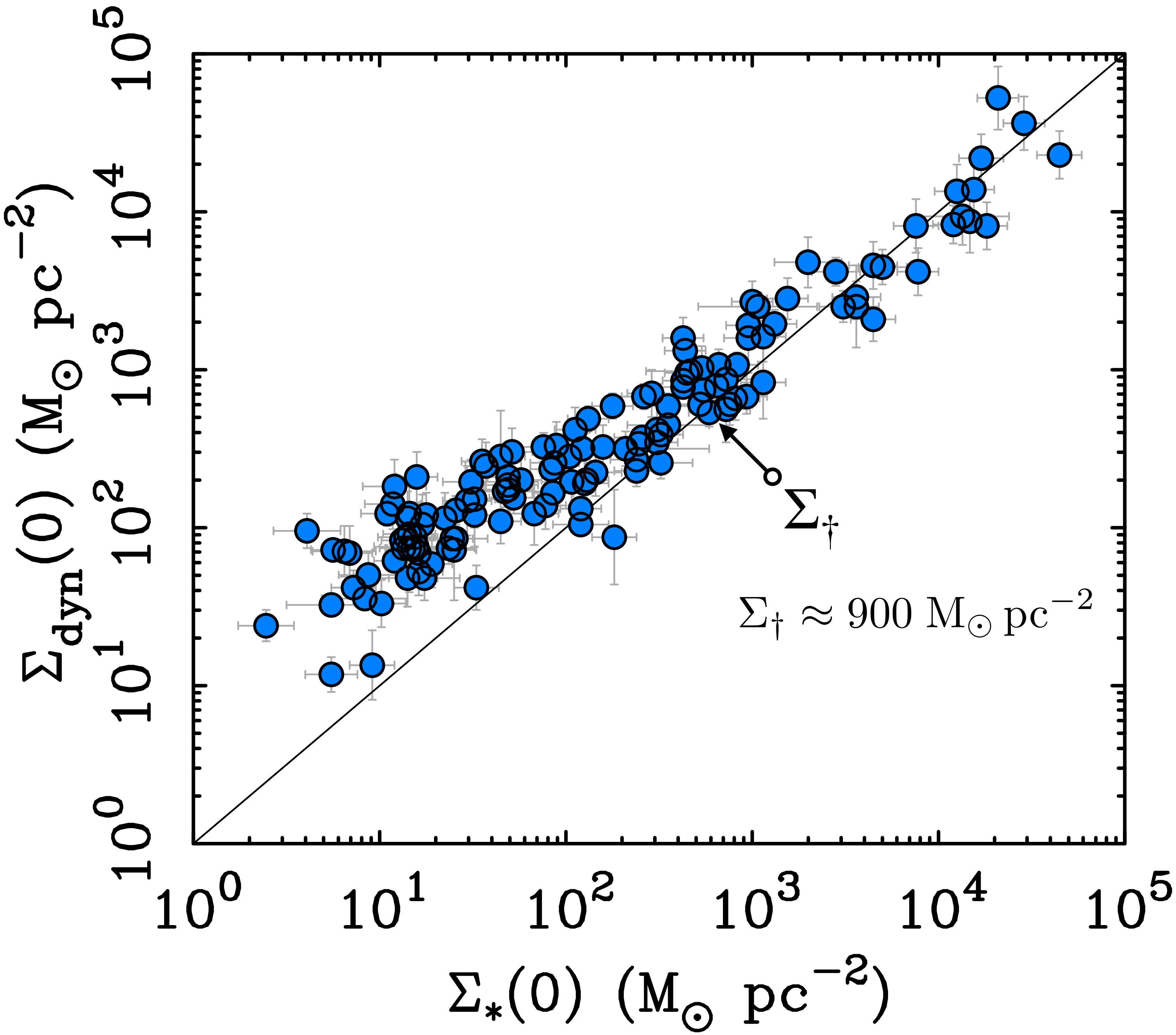

central surface brightness